Odensjön – A new varved lake sediment record from southern Sweden

Hanna Hertzman

Dissertations in Geology at Lund University,
Master's thesis, no 611
(45 hp/ECTS credits)

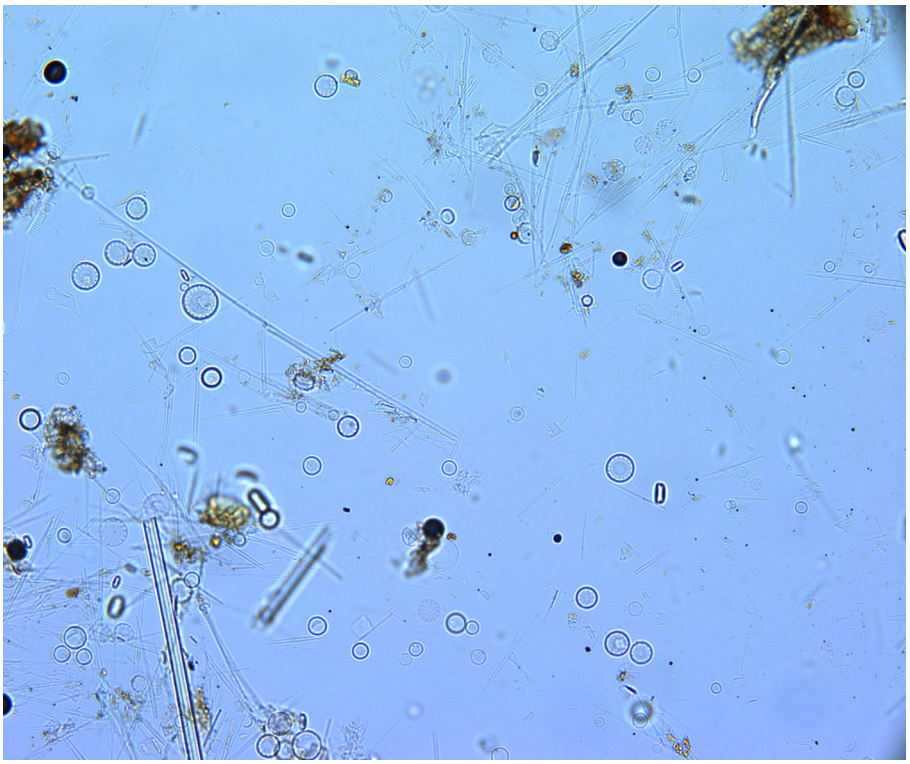

Department of Geology
Lund University 2021

Odensjön – A new varved lake sediment record from southern Sweden

Master's thesis
Hanna Hertzman

Department of Geology
Lund University
2021

Contents

Cover Picture: Hanna Hertzman, 2018

Abstract

HANNA HERTZMAN

Hertzman, H., 2021: Odensjön – A new varved lake sediment record from southern Sweden. *Dissertations in Geology at Lund University*, No. 611, 26 pp. 45 hp (45 ECTS credits).

Abstract: Annually laminated (varved) sediments provide opportunities to reconstruct climate change and human impact on the environment with high temporal resolution. Depending on the character of the varves, such sediments can provide insight into the delivery of both autochthonous and allochthonous material from the lake and its catchment and answer questions regarding both regional and local responses to climate- and land-use changes. This thesis examines a new sediment record from the small Lake Odensjön in southern Sweden. The aim of the study is to describe the sedimentary sequence, determine the type of laminations and establish if these are annual, and to date the sediment sequence using radiometric methods together with varve counts. The uppermost 910 mm of the sediment sequence was collected with a freeze-corer at 20 m water depth in the deepest part of the lake. Dating with ^{210}Pb and ^{137}Cs in combination with identification of the distinctive and well-documented pollution Pb peak associated with the use of leaded petrol in the mid 1970's confirms that the sediments partly consist of laminations representing annual varves. Radiocarbon dating of the lower part of the record demonstrates its extension to around 450 years before present. The sediments are characterized by X-ray fluorescence, biogenic silica content, total carbon and nitrogen content and microscopic analyses are showing high contents of biogenic silica and organic matter, abundant diatoms and low minerogenic content, demonstrating that the varves are of biogenic origin and annual. The varve counting was limited by thin and indistinct layers in part of the core. The conditions for varve formation have changed through time and substantial variations in the content of macroscopic plant remains give evidence of pronounced changes in catchment land-use. In the late 19th century the catchment most likely was completely deforested, while rapid colonization by beech, *Fagus sylvatica*, occurred during the following century as demonstrated by abundant well-preserved leaves.

Keywords: Varved lake sediment, late Holocene, organic sediments, diatoms, land-use history, southern Sweden, palaeolimnology

Supervisors: Karl Ljung and Dan Hammarlund

Subject: Quaternary Geology

Hanna Hertzman, Department of Geology, Lund University, Sölvegatan 12, SE-223 62 Lund, Sweden. E-mail: hanna.hertzman@gmail.com

Svensk sammanfattning

HANNA HERTZMAN

Hertzman, H., 2021: Odensjön – ett nytt varvigt sjösediment från södra Sverige. *Examensarbeten i geologi vid Lunds universitet*, Nr. 611, 26 sid. 45 hp.

Sammanfattning: Varviga sediment utgör unika högupplösta klimat- och miljöarkiv som ger oss möjligheter att rekonstruera klimatförändringar och mänsklig påverkan på miljön. Genom varvens karaktär och genom sedimentet kan vi få insikt i hur både autoktont och alloktont material, det vill säga både material från sjön och från avrinningsområdet, och detta kan i sin tur ge information om både regionala och lokala förändringar till följd av förändrad markanvändning och klimatologiska förhållanden. Här presenteras ett nytt sedimentarkiv från en liten dimiktisk sjö, Odensjön i Skåne, södra Sverige. Syftet med studien är att avgöra vilken typ av laminering som sedimenten är uppbyggda av och om lamineringen är årlig, samt att datera sedimenten med hjälp av radiometriska metoder och varvräkning. Två fryskärnor har tagits upp från den djupaste delen av sjön på 20 meters vattendjup. Dessa kärnor omfattar de översta 91 cm av sedimentet i sjön. Datering med hjälp av ^{210}Pb och ^{137}Cs i kombination av identifiering av förhöjda bly-värden under mitten av 1970-talet till följd av användningen av bly i bensinen har kunnat användas för att klargöra att den översta delen av kärnan består av årliga lamineringar, alltså ett varvigt sediment. ^{14}C datering av den nedersta delen av kärnan gav resultatet att hela kärnan är ungefär 500 år gammal. XRF, BSi, C:N förhållanden och mikroskopanalyser av sedimentet har visat ett högt innehåll av biogent kisel samt organiskt material, högt innehåll av kiselalger och ett lågt innehåll av minerogent material har visat att sedimentet och varven är avsatta av biogena processer. Förhållandena för varvbildning har förändrats över tid och väsentliga skillnader i andelen avsatta makroskopiska växtdelar ger oss indikationer på stora förändringar i markanvändningen i sjöns avrinningsområde. Vid 1800-talets mitt var avrinningsområdet förmodligen helt avskogat och under det följande århundrandet så har återkoloniseringen av bok, *Fagus sylvatica* varit snabb och omfattande. Detta representeras i kärnan av ett stort innehåll av välbevarade löv från 1900-talets början tills idag. Detta nya varviga sediment representerar det sydligaste i Skandinavien av sitt slag, sedimentet kommer att fortsätta att analyseras med en rad olika metoder och resultera i en djupare förståelse i hur miljö- och klimatförändringar har påverkat södra Sverige.

Nyckelord: Varviga sjösediment, sen Holocen, organiska sediment, diatomer, landskapshistorik, södra Sverige, paleolimnologi

Handledare: Karl Ljung och Dan Hammarlund

Hanna Hertzman Geologiska institutionen, Lunds Universitet, Sölvegatan 12, 223 62 Lund, Sverige. E-post: hanna.hertzman@gmail.com

1 Introduction

Sediments deposited in water, weather it is in marine or lacustrine settings hold information about past environmental changes (Ojala et al. 2012).

Varved sediments are useful arcives for understanding and investigating both local and regional climate change and ecosystem responses to human impact and land-use changes in the past (Brauer, 2004; Ojala et al. 2012; Randsalu Wendrup et al. 2012; Tylmann et al. 2013; Zolitschka et al. 2015). The great advantage with varved sediments is that past environmental changes can be reconstructed with high temporal resolution and precision. There are fundamental requirements for the formation of varved sediments in lacustrine environments. Firstly, there needs to be a seasonal variation in the chemical processes, biological activity and the input from the terrestrial surroundings. Secondly, that the varves are formed under conditions that are preserving them, i.e. anoxic bottom waters with no or negligible bioturbation (Zolitschka, 2007).

In Europe, varved sediments are mostly found in formerly glaciated northern and central regions. In Sweden approximately 100 lakes with varved sediments have been found, predominantly in the central and northern parts of Sweden. (Petterson, 1996).

This thesis will focus on Lake Odensjön in southern Sweden. According to Rapp (1988) the uppermost 5.5 m deposits of lake Odensjön consists of varved gyttja down until an age of late Younger Dryas. The varved sediments in Lake Odensjön have not been described in detail until now. **Therefore, the aims of this study is to describe the sediments, what they consist of and how they are build. Further, the aim was to identify if the varves are annually formed and what processes that contribute to the formation of the varves.** The sediments provide a new and important palaeoenvironment and palaeoclimate record. It is likely the most southerly lake with varved sediments in Sweden.

This thesis is focusing on the following questions:

- **What kind of sediment constitutes the varved sequence from Lake Odensjön?**
- **Do the laminae build annually forming varves?**
- **How old is the sediment sequence?**

2 Study area and site description

Lake Odensjön is located in the northwestern part of the southernmost province of Sweden, Scania (56° 0'13.96"N, 13°16'32.27"E, at 60 m asl, Fig. 1).

It is situated on the east side of one of the horst ridges, Söderåsen, that runs across Scania in a north-west-southeast direction. The lake is small with a diameter of appr. 160 m and a maximum depth of around 20 meters. It is surrounded by steep talus slopes reaching 30 m above lake level. According to Rapp (1984) Lake Odensjön was formed by a glacier niche during tundra periods before and after last glaciation. Odensjön has the typical features of nivation with a hollow in bedrock and a semicircular back rim, a floor that has a gentle slope and angular rock debris covering the floor and sides (Berglund and Rapp, 1988, Fig. 2). The lake is drained through a wetland to the north of the lake.

Fig. 1. Location of Lake Odensjön in Sweden.

The bedrock surrounding Lake Odensjön comprise primarily of Precambrian gneiss. Soils in the direct surroundings contain angular blocks and talus,

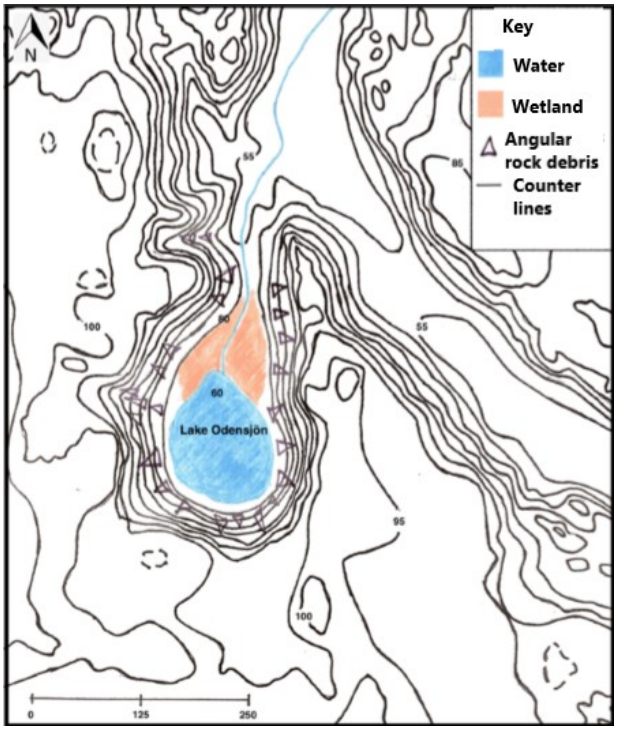

Fig. 2. Geological map of the area around Lake Odensjön. 5 m between counter lines. The figure is modified from Berglund and Rapp (1988)

partly covered by peat (SGU, 2019: Fig. 3) The climate in the area is influenced by the proximity to the west coast. The mean annual air temperature is 7.7° C and the mean annual precipitation is 687 mm (at the closest weather station, Svalöv at a distance of 16 km, for the period 19611990, SMHI 2018 a and b). Today the landscape in the direct vicinity of the lake is mainly covered by *Fagus sylvatica,* with some minor occurrence of *Alnus glutinosa* and *Betula pendula.* Above the talus slopes surrounding the lake *Picea abies* has been planted.

Regarding the historical land-use around the lake there is not much literature describing the direct surroundings of the lake. Historical maps of the area from the time period AD 1717 to 1915 describe the steep talus slopes surrounding the lake as "unusable land" (Lantmäteriet, 2018).1 However, there are some literature describing the land-use history of the whole area of Söderåsen (Håkansson, 1948; Persson, 1971). The oldest map of the Söderåsen area was constructed by Gerhard Buhrman, AD 1684 (Håkansson, 1948). On this map, most of the forest is described as dominated by *Fagus* and the surrounding plains were open farmland (Persson, 1971). At this time, the Swedish Crown, i.e. the state, owned the silviculture except for *Alnus, Betula, Salix* and *Corylus* that was growing on the wetlands (Håkansson, 1948). These species were allowed to be used by the farmers. It was not until AD 1793 when the taxpaying farmers were allowed to use the forest, including the *Fagus* but it was still owned by the state (Persson, 1971). At this time the forest was mainly used for grazing by cattle, horses and pigs (Håkansson, 1948). In the beginning of the 19th century deforestation started, and a more open landscape was created on the Söderåsen Ridge. During this time, the *Laga skifte* was implemented. Laga skifte was a land reform where the Crown's forest was devolved to private owning and a more effective agriculture took form. As a consequence of this, deforestation intensified and the area of Söderåsen was as most open during the 1850's. The agriculture was further intensified with the help of industrially produced fertilizers. This led to reduced pressure on the forest due to less grazing because the farmers used less land to produce feed for the animals. The replanting of the area started in AD 1875. The open landscape was replanted with *Picea* and some of the *Fagus* was replaced by *Picea* (Persson, 1971). The only animals that were still grazing on the Söderåsen Ridge were pigs, until the 1930's.

3 Materials and Methods

3.1 Sediment coring

Two cores were extracted with a freeze corer from lake ice in January 2016. The cores were extracted from the deepest parts of the lake, one at 19.9 m and the other at 18.8 m depth. For this thesis the core from 19.9 m depth was used for analyses. The core was wrapped in plastic and kept frozen at -18 °C before subsampling.

3.2 Subsampling and documentations , :

Photos were taken throughout the sediment core to be

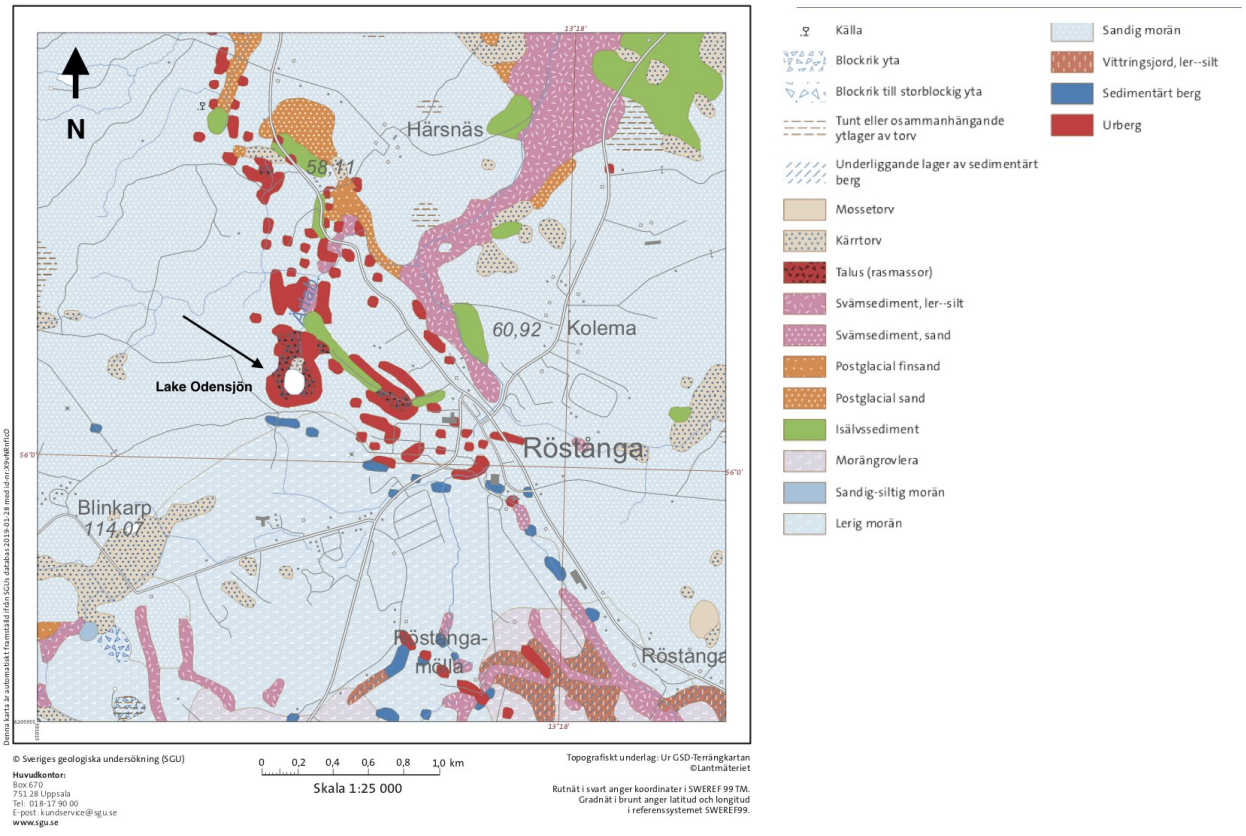

Fig. 3 Map of soils in the surrounding. Lake Odensjön is marked with an arrow. SGU, 2018a.

for documentation of the core and to be used for counting the laminae. The subsampling and photo documentation were done in a freezer room to make sure the sediments were kept frozen for further analyses. Photos were taken on the still frozen core to prevent reactions, oxidation and colour changes of the sediment caused by thawing.

3.3 Lithostratigraphic description

The core is 910 mm long and consists of more or less visible laminations. Light and dark laminae are visible and the general colour is changing throughout the core. As seen in Fig. 4, the brown colour is changing from light reddish brown in the very top of the core to a more dark brown colour at a depth of approximately 250 mm to 340 mm. Thereafter the colour is again more reddish brown down to a depth of around 800 mm where the colour is again changing to darker variation of brown. The laminations mostly consists of material of organic origin.

3.4 Varve counting

The laminae were counted from highresolution pictures that were taken in the freezer room. The laminations throughout the full core were counted three times. The pictures were used both as a printed version and digitally so that the colour settings could be changed to visualize the laminae in the best possible way.

3.5 Radiocarbon and ^{210}Pb dating

To date the sediment we used ^{210}Pb dating and radiocarbon dating. The uppermost part of the core was ^{210}Pb dated and the lower part radiocarbon dated using macrofossils. Along with the counted laminae the purpose of using these techniques was to achieve a chronology as detailed as possible.

For ^{210}Pb dating, the top 33 cm of the core was cut in 2 cm subsamples. The uppermost sample was cut in a 4 cm subsample due to the high water content. The samples were freeze-dried and analyzed for ^{210}Pb, ^{226}Ra, ^{137}Cs and ^{241}Am at the Environmental Radiometric Facility at University College London.

Three samples were taken for ^{14}C dating. Macrofossils of leaves from the depths of 687, 760 and 885 mm were used for the analyses. The samples were treated with HCl and NaOH prior to analysis. The analysis was performed at the Radiocarbon Dating Laboratory at Lund University.

3.6 Wiggle-matching

The calibration of the ^{14}C dates was preformed using OxCal v.4.3.2 Bronk Ramsey (2008). Calibration of the radiocarbon dates were done using both D-sequence and P-sequence. D-sequence was used to wiggle match the radiocarbon dates. D-Sequence is a wiggle matching method using the number of varves (years) between ages to constrain the calibration. P-Sequence is a less rigid model based on the assumption of stratigraphic order of the radiocarbon dates. Because of a large uncertainty in the number of laminations between the two lowermost dated horizons the radiocarbon ages were also calibrated using P-sequence. The final age-depth model was constructed using the information from the ^{210}Pb dates and ^{14}C dates calibrated using P-sequence, and not the information from the lamina counting. The information from the lamina counts was excluded because of the uncertainty of the lamina counting between two ^{14}C dates in the lower part of the core.

3.7 XRF-analysis

The XRF analysis were done for the purpose of finding in lamina elemental variations that could answer questions about the formation processes forming the laminae. The XRF analysis was performed at the Centre of GeoGenetics at the Natural History Museum of Denmark in Copenhagen. An Itrax Core Scanner was used with a Rhodium tube. The exposure time was set to 2 seconds with 100 microns resolution. The initial spectra were scanned with a step size of 0.1 mm i.e one data point per 0.1 mm, this was done to be able to reconstruct variantions on varve-scale and use the elemental composition for counting varves. To increase the signal strength the spectra were later added up to 1 mm resolution. The results are given in counts per second (c/s) which is the intensity of X-rays as a function of the energy emitted from one data point (Croudace & Rothwell, 2015) The XRF analysis was done down to a depth of 880 mm (of the total 910 mm). The core was cut into subsamples in the freezer room to keep them frozen for the analysis. The XRF sections were cut in approximately 160 mm slabs with overlaps of ~40 mm. The length of the XRF sections was kept short to minimize thawing during the XRF scanning. The XRF sections were packed in Styrofoam boxes to reduce thawing and the samples were taken out of the freezer just before analysis and covered with plastic film. The Fe curve and the high resolution pictures were used for correlation of individual sections. However, some limitations using the Fe curve have to be considered. The laterally overlapping slabs, and their laminations do not look the same when moving a few centimeters to the side on the core. Therefore, features of the core such as laminae and macrofossils were used to visually fit the slabs and to obtain a continuous Fe record.

3.8 Biogenic Silica

To measure the biogenic silica (BSi) concentration in the sediment a sequential alkaline extraction method described by DeMaster (1981) was used. 30 mg of sediment from each cm of the core was freeze-dried, homogenized and mixed with 40 ml of 0.1 M Na2CO3, and then put in a shaking water bath at 85°C for 5 h. Thereafter an aliquot was subsampled after 3, 4 and 5 h of reaction and neutralized with 9 ml of 0.021 M HCl. The dissolved Si (DSi) was measured with a SmartChem 200 discrete chemical analyzer using the molydate-blue methodology (Eggimann et al. 1980). Lastly the BSi concentrations were calculated by determining the intercept of the regression between total extracted Si and extraction time (Conley, 1998; Sauer et al 2006). **This method was used to answer questions about the laminae, what they consists of and how they are formed.**

3.9 Bulk carbon and nitrogen analyses

Total organic carbon (TC) and total nitrogen (TN) contents were measured on samples taken every second cm down to 880 mm of depth. **To answer questions about the laminae and what the sediment consists of macrofossils were avoided during sampling. This was done to avoid results showing the TC and TN of the macrofossils themselves instead of the sediment.** Approximately 3 mg of freeze dried sample material was loaded into Sn-capsules before measurements. The analyses were performed on a Costech ECS4010 at the Department of Geology, Lund University.

The results from the analysis of the carbon and nitrogen content of the sediment were multiplied with 1.167 to get the atomic ratios. The variation of C:N atomic ratio within lake sediment can be used to determine the source of organic matter to the lake. Generally, algal organic matter has lower ratios, between 4-10 and terrestrial organic matter have C:N ratios greater than 20 (Meyers, 1994).

3.10 Smearslide analysis

Samples for smear slides were taken from both dark and light layers, **with the aim of identifying lithological differences and to study the differences between the light and the dark laminae.** A semi-quantitative approach was used for this analysis and a small amount from each layer was added into 1.5 ml of deionized water and put in an ultrasonic bath for 1 minute to break up aggregates. 200 µl of the solution was transferred to an object glass and fixed with Naphrax. Each sample was analysed under light microscope at 10x40 times magnification. The following material classes were identified and counted; mineral particles, detritus, cellular fragments, charcoal fragments, Daphnia, and diatoms. The diatoms were further divided into the following morphological classes centric-, pennate- and oval- shaped diatoms, and one class for other shapes of diatoms. Furthermore, the diversity in the class "other shapes" was noted while counting.

5 Results

5.1 Description of the core

The full core was 910 mm in total. The characteristics, structure and colour of the sediments change throughout the core and to facilitate the description of the core and its characteristics the core was divided into six different sections. The sections are named S1, S2 and so on. Each section (Sx) contains further 'undefined' subsections (HSx), shown in Fig. 4 and Table 1. These sections are called undefined because the laminae have been difficult to distinguish within these sections. Some of them contain laminae that are visible to the naked eye whereas others appear to consist of more or less homogenous detritus gyttja. Section 1 (0-270 mm, hereafter S1 etc, Fig. 4) has well-defined and less consolidated laminae than further down the core, i.e the laminae are here less compacted. When this section was thawed it shrunk to almost half its original size due to the high water content. The laminae in this section are generally thicker (2-4 mm) than in sections further down the core (1-5mm), The section has on

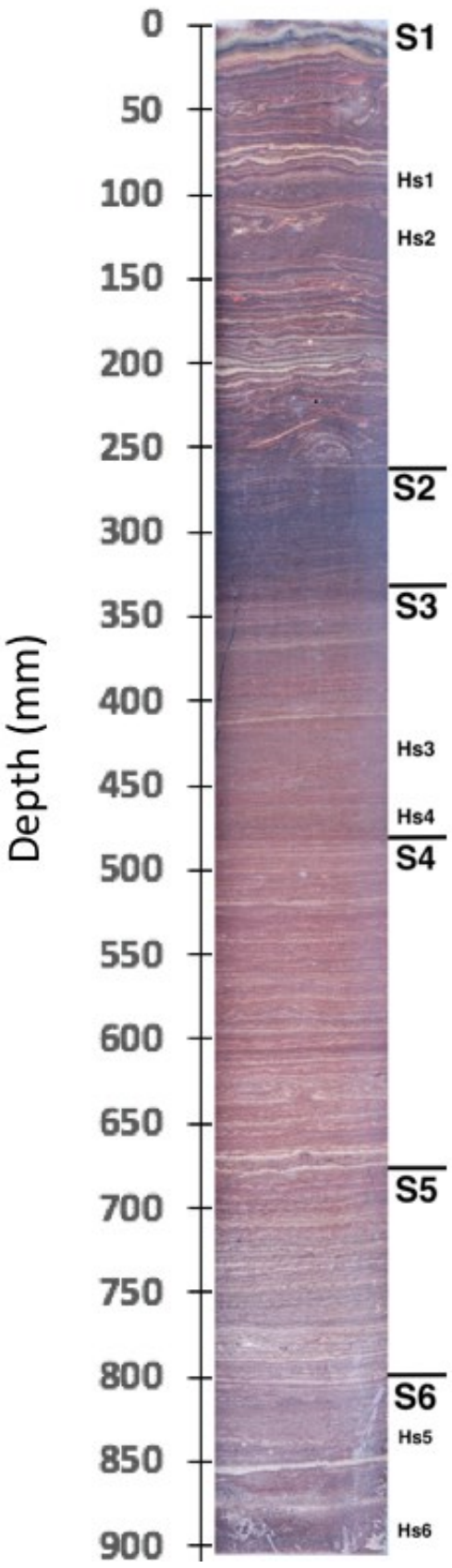

Fig. 4. Full core of Lake Odensjön with markers for sections described in table 1 and text.

Table 1. Sections of the core and their ages and depths.

Section, S	Undefined sections , HS (Within section X)	Depth (mm)	Number of lamina/cm	Age AD
S1		0-270	2,52 (68/27)	2017-1936
	HS1 (S1)	~ 99-109	-	2002-2000
	HS2 (S1)	~118-141	-	1998-1993
S2		270-346	4,66 (27/6)	1928-1869
S3		346-484	3,38 (48/14,5)	1869-1760
	HS3 (S3)	~ 425- 448	-	1806-1788
	HS4 (S3)	~ 470-484	-	1771-1760
S4		484-683	4,7 (97/20,5)	1760-1603
S5		683-812	6,75 (81/12)	1603-1527
S6		812-910	0,9 (11/10)	1527-1479
	HS5 (S6)	~ 818-862	-	1524-1503
	HS6 (S6)	~ 866-910	-	1497-1479

Fig. 5. Photo taken just after coring, the sharp boundary between a great abundance of leaves and almost no leaves is clear.

average 2.5 laminae per cm (Table 1). Two undefined subsections are found in S1, HS1 and HS2 at 99-109 mm and 118-141 mm, respectively (the undefined sections, HSx, are listed in Table 1 and marked on Fig. 4) S1 has a high content of macroscopic plant remains. Most of the plant remains are leaves of *Fagus* (Fig. 5) and a few *Alnus* and *Betula* were observed. The boundary between where leaves were found (in great abundance) and almost no leaves is very sharp, at a depth of approximately 270 mm. This is also the boundary between S1 and S2. The section below, S2 has a darker colour and less well-defined laminae. In this section the laminae were very difficult to distinguish and count, mostly due to the thin and dark-coloured laminae, less than 1 mm or thinner. It was possible to distinguish approximately four laminae per cm (Table 1), but these were all thinner than 1 mm. Therefore, there are probably laminae that were not possible to distinguish in this section. Scattered *Fagus* sylvestris leaves were found throughout the section. In the next section, S3, the colour changes to more red-

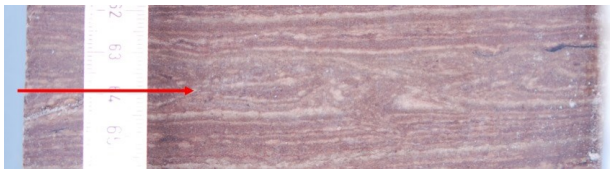

Fig. 6. Figure showing probable gas escape during and after sedimentation of laminae at depths of 630 to 645 mm.

dish brown and the number of laminae per cm is on average 3.4. Two undefined subsections were found, HS3 and HS4. The macroscopic plant remains found were dominated by *Fagus* spp leaves. S4 is the longest section, spanning from 474-673 mm of depth and here the laminae are well-defined, compared to S2. The lighter laminae are lighter than in S3. Between 630 and 645 mm depth a section with disturbed laminae was found, the disturbed laminae may be due to gas escape (Fig. 6). During subsampling and thawing of the samples gas bubbles were seen escaping from the sediments. The gas was probably methane, but the smell also indicated presence of hydrogen sulfide. Three laminae with greater thickness than average of the section were found with a thickness of around 3 mm at depths of 526, 604 and 677 mm respectively. The average number of laminae per cm is 4.7. The macro-fossils identified were mainly *Fagus leaves.*

Further down, in S5, the colour changes to darker brown and the laminae are welldefined. This section represents the part of the core with the thinnest countable laminae, with 6.75 laminae per cm. As well as in the previous section, this section contains a number of thicker laminae with a thickness of 2-3 mm (at depths of 686, 780 and 795 mm). The macro-fossils found here were leaves of *Betula.* The last section S6 has a dark brown colour and the upper 45 mm part of this section consists of homogeneous detritus gyttja, HS5. The thickest lamina found in the consolidated part of the core was situated at 860-865 mm of depth with a thickness of 5 mm. Only 11 laminae were visible over 100 mm. The lowermost part of the analysed core (below 880 mm of depth) consists of homoge-

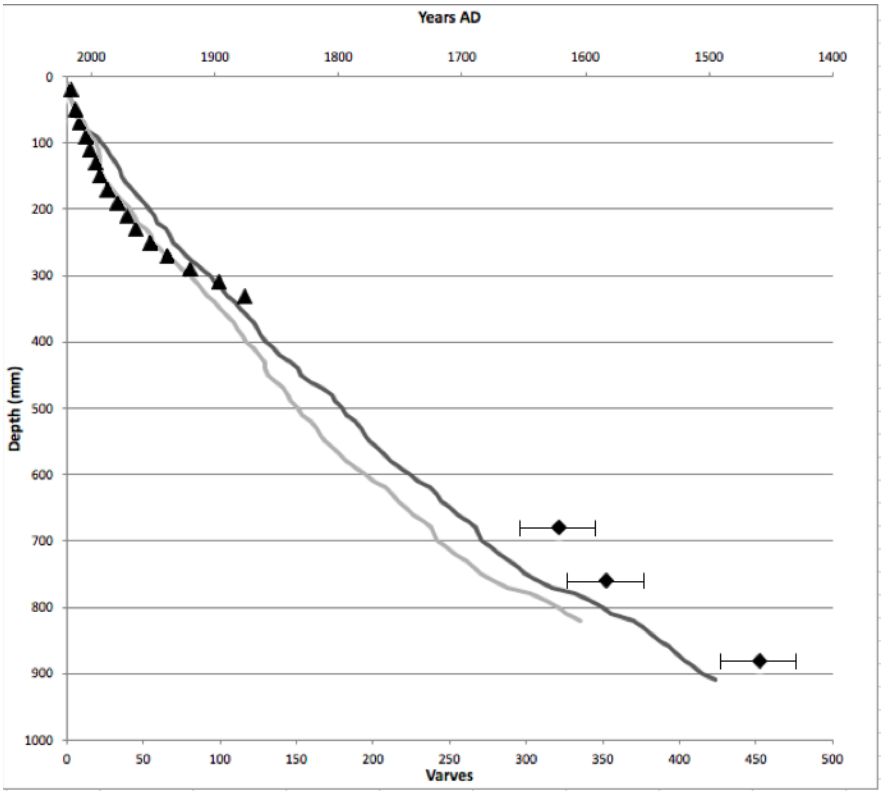

Fig. 7. Graph showing counted laminae.. The light grey solid line represents the counted laminae where the undefined subsections are considered as one laminae. The dark grey solid line represents the counted laminae with the extrapolated laminae in the subsections. The triangles represent the Pb-dating and the squares represent the carbon 14– dating with error bars.

Table 2. Age distribution derived from 210-Pb dating

Depth	Dry mass	Chronology		
cm	g cm^{-2}	Date AD	Age yr	±
0	0	2017	0	
2	0.0161	2016	1	2
5	0.0663	2013	4	2
7	0.1145	2009	8	2
9	0.1716	2005	12	2
11	0.2328	2001	16	2
13	0.2905	1997	20	2
15	0.3577	1993	24	2
17	0.4391	1987	30	2
19	0.5283	1979	38	2
21	0.6193	1971	46	2
23	0.7083	1964	53	2
25	0.8084	1953	64	3
27	0.9154	1938	79	4
29	1.0215	1920	97	5
31	1.1231	1897	120	9
33	1.2155	1876	141	16

nous detritus gyttja, HS6. Macro-fossils found at this depth were leaves of *Betula* spp. and *Corylus* spp.

5.2 Chronology

The chronology of the core is based on independent dating using ^{210}Pb, ^{14}C and lamina counting (Fig. 7). The lamina counting was done from top to bottom and performed three times. The total number of visible laminae was determined to 339 (Fig. 7). At first, the undefined subsections of the core were counted as single laminae. However, as the undefined sections probably represent more than one year an estimation of the number of laminae within the undefined subsections was done after the first counting. The undefined subsections were compared with the closest centimeters (with lamination) situated above and below these sections. The average number of laminae per cm was then extrapolated to the undefined subsections. The result after these tentative additions gave a total number of 423 laminae (Fig. 7).

^{210}Pb dating was done down to a depth of 330 mm (Fig. 7). The chronology and sedimentation rates were calculated using the constant rate of ^{210}Pb supply (CRS) dating model (Appelby and Oldfield, 1978; Appelby, 2001). **In this chronology, the year 1963 and 1986 were placed at depths of around 230 and 170 mm, respectively using the information obtained from the samples representing the depths from the ^{210}Pb dating (Table 2).** These depths represent the peaks in both ^{137}Cs and ^{241}Am from the artificial fall-out of radionuclides from the testing of nuclear weap-

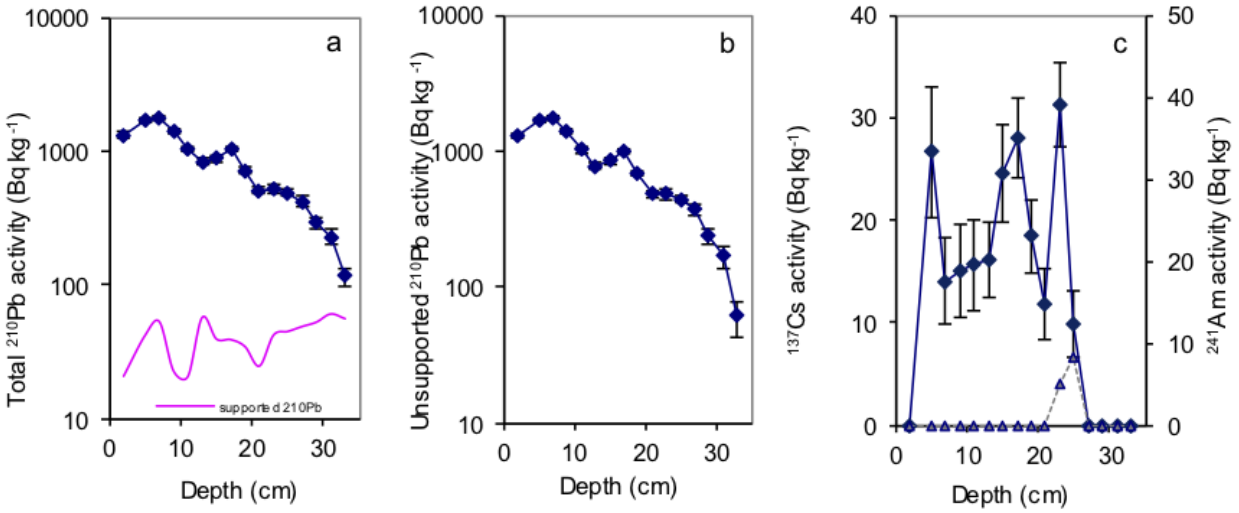

Fig. 8. Fallout radionuclide concentrations in the core taken from Lake Odensjön, showing (a) total 210Pb, (b) unsupported 210Pb, and (c) ^{137}Cs and ^{241}Am concentrations versus depth.

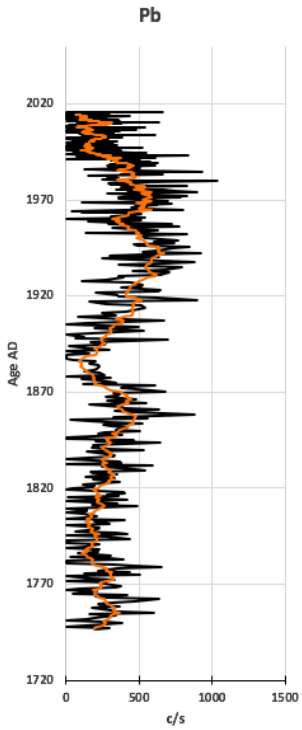

Fig. 9. Lead distribution in the core during the last 300 years. A peak is seen during the 1970's and after this a general decrease in the Pb c/s. The orange solid line is a 10

Table 3. The depth and the type of microscopic plant remains used for radiocarbon dating and thereof obtained ages.

Sample name	Lab no	Depth (mm)	Dated material	Obtained ^{14}C age
Ac5	LuS 13481	687	*Fagus* leaf	340 ± 40
Ac21	LuS 13482	760	Leaf fragment	430 ± 40
Ac25	LuS 13483	885	*Betula* leaf	430 ± 40

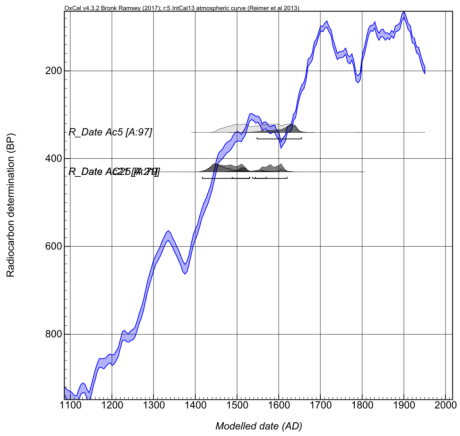

Fig. 10. Calibration curve for the radiocarbon dates

Table 4. Information from the wiggle matching with D_sequence and the P_sequence with depth as prior.

Depth (mm)	Type of sequence in OxCal	Modelled (BP) From	To	Year AD	Agreement index
687	D-sequence	357	300	1622	95.8
687	P-sequence	403	296	1601	96.6
760	D-sequence	396	399	1583	19.2
760	P-sequence	462	311	1554	21.3
885	D-sequence	520	463	1549	119.1
885	P-sequence	534	381	1488	79.1

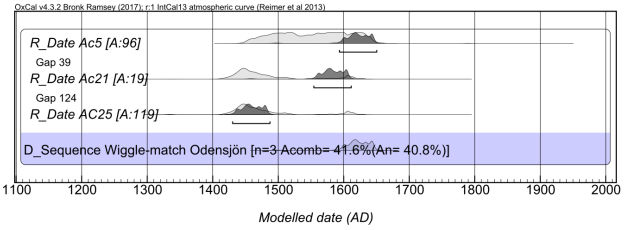

Fig. 11. D_Sequence wiggle match and the calibrated ages.

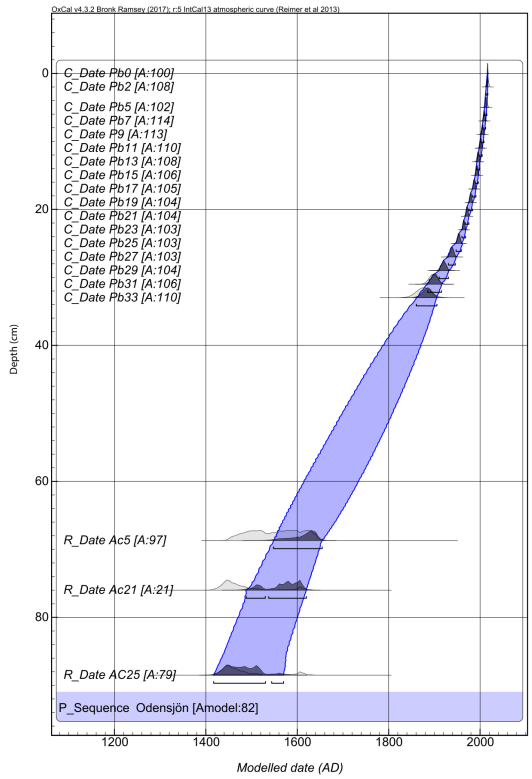

Fig. 12. P_sequence model.

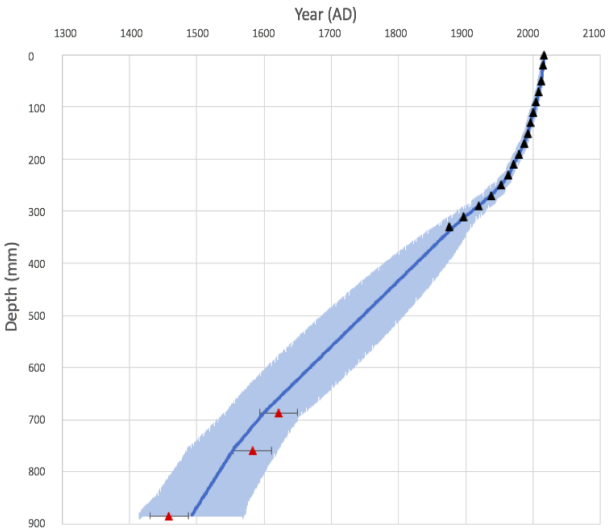

Fig. 13. Final age model based on information from the P_sequence obtained in OxCal. The black triangels are 210Pb dates. The red triangles are radiocarbon dates calibrated using D-sequence. The blue line is the model obtained from the P_sequence with two sigma standard deviation in shaded blue.

ons (corresponding to peaks around AD 1963) and the Chernobyl accident (AD 1986), respectively (Hardy, 1977; Cambray et al. 1987, Fig. 8).

As shown in Fig 7, the number of visible laminae fits well with the ^{210}Pb dating, down to approximately 270 mm. Below this depth the number of visible laminae and the ^{210}Pb dates diverge.

The ^{210}Pb dating is corroborated by a peak in the Pb results from the XRF at around 200 mm, which represent the elevated pollution lead deposition during the 1970's as a result of extensive use of lead in petrol (Smol, 2008, Fig. 9).

The lower part of the core was radiocarbon

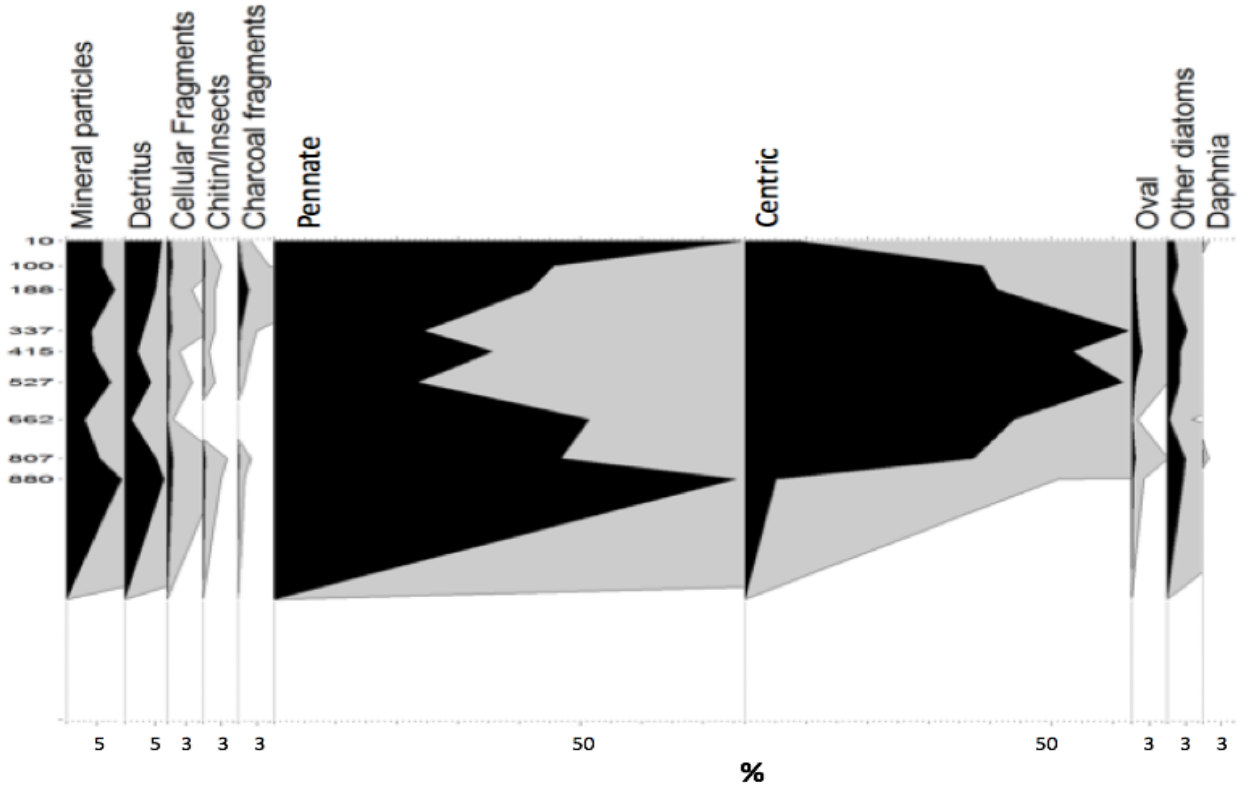

Fig. 14. Records of different morphological classes identified in smear -slides. The dominant classes are pennate and centric diatoms.

dated (Table 3). ^{14}C-dating was done at depths of 687, 760 and 885 mm. The dating at depths of 760 and 885 mm gave the same age. The radiocarbon dates were calibrated using both wiggle matching (D-sequence) and only the depth as prior (P-sequence). The radiocarbon ages fall on a section of the calibration curve with large shifts that can be used to give good wiggle matching provided the age gaps between dated levels are known (Fig. 10).

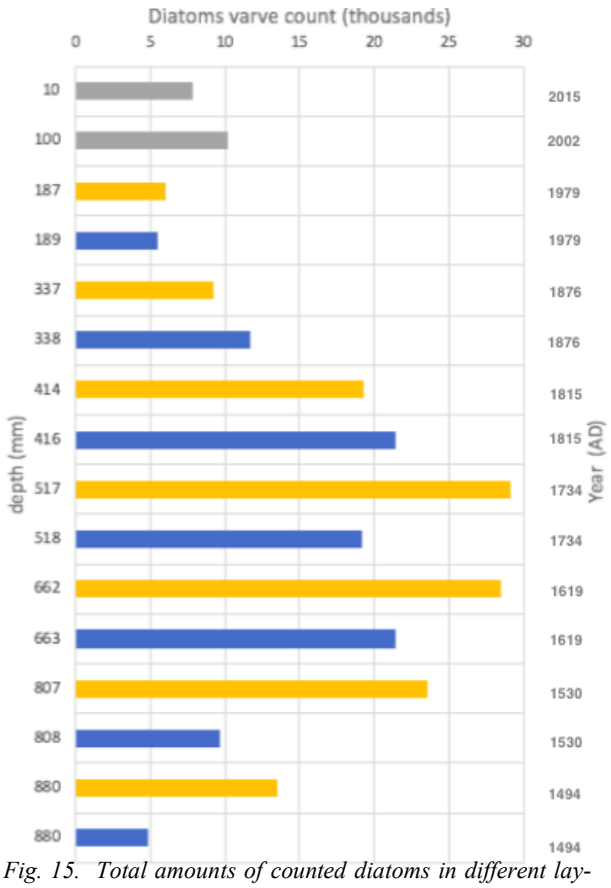

Fig. 15. Total amounts of counted diatoms in different layers. For each depth (except the uppermost two samples), one light (yellow) and one dark lamina (blue) were analysed.

Because of the undefined subsections between 818 and 862 mm (HS5) and between 866 and 910 (HS6) the number of laminae between the depths of 760 and 885 mm are uncertain. The average number of laminae between 760 mm (AD 1583) and 885 mm (AD 1489) is therefore uncertain, and the radiocarbon ages were calibrated using only depth as prior.

For the wiggle match, D-sequence in OxCal v 4.3.2 was used (Fig. 11 and Table 4). The number of laminae is 50 between 687 mm and 760 mm and 124 between 760 and 885 mm. This assumes that the undefined sections are not representing one event i.e one deposition event but instead they have been deposited with the same sedimentation rate as above, just without visible laminations. The results show an overall agreement index of 41 %. The agreement index is used as a way to evaluate the model statistically (Ramsey et al 2001, Table 4). This is lower than the suggested 60 % agreement index for a reliable calibration. The radiocarbon age at 760 mm has a low agreement index of 19 %, which is well below the cut off (Table 4). This indicates that this age is erroneous and too old rather than the date below being too young. This is probably due to re-deposition of plant remains within the catchment. There might have been old leaves in other parts of the catchment that have been redeposited to where they are found today. Due to the fact that the core is laminated, younger material cannot have moved within the core because of bioturbation or other processes.

The radiocarbon ages were further calibrated using the P-sequence, **a more conservative model,** which only uses depth and assumptions on sedimentation

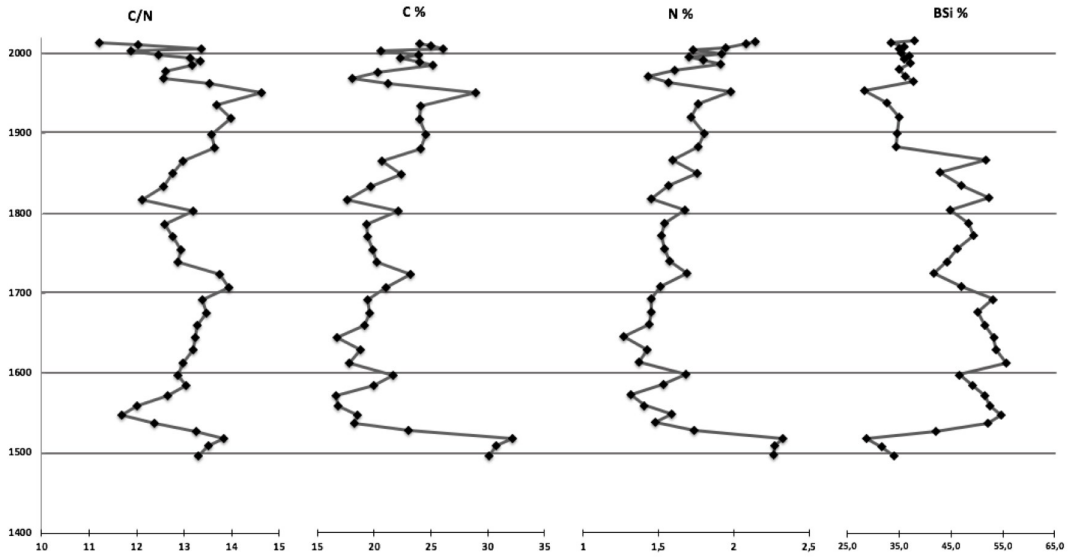

Fig. 16. Graph showing Total C, Total N and the C:N ratio as well as the results from the BSi

as prior information. The P-sequence was run with the depths of the radiocarbon dates and the ^{210}Pb ages. The k-value was set at 1 (cm). The overall agreement index for the P-sequence is 82 % (Fig. 12). The radiocarbon date at 760 mm has an agreement index of 21 %, indicating that the obtained age does not fit well with the model (see Table 4). The D-sequence procedure gave different ages, but within the error estimates, than the calibration using P-sequence (Table 4). Both methods show that the date at 760 mm fits the model poorly, and likely is too old. Because of the uncertainty in the number of lamina between the lower two radiocarbon dates the more conservative P-sequence model is used for the final age model (Fig. 13).

5.3 Smear-slides

Out of the different classes of material that were identified during smear-slide analysis, the highest numbers were found in the pennate and centric diatom classes (Figure 14).

Therefore, the sediments and laminae are considered to be biogenic. There were also minor portions of mineral particles, detritus and cellular fragments (Fig. 14). Thus, most of the sediments in Lake Odensjön have an autochthonous origin. However, the mineral particles are allochthonous and some of the detritus and cellular fragments could have an origin from the surrounding environment. When only the number of diatoms is studied, and the dark and light laminae are compared the results show that there are in general more diatoms in the light layers than in the dark laminae (Fig. 15). The light lamina (yellow in graph) have a greater total amount of diatoms than the dark lamina (blue in graph).

The two top samples were mixed samples (green in graph), i.e. the samples were taken from a bulk sample and therefore mixed with both light and dark laminae from one cm. The highest amounts of diatoms were found between 662 and 517 mm depth (AD 1734 – 1619), which coincides with the maximum content of biogenic silica (Fig. 16). The smallest number of counted diatoms was found at the depth of 187189 mm (AD 1978). However, the uppermost sample is not really comparable with the rest of the samples because this samples was mixed and is representing a bulk sample from 10 mm of the core. As the absolute abundance of diatoms falls from a depth of 414 mm towards the top.

Figure 14 shows the distribution of all identified morphological classes of combined smear-slide data from dark and light layers. The data show a simultaneous increase in the centric morphological group and a decrease in the pennate group beginning at 807 mm (AD 1530) and the trend is again shifting towards an increase in pennate diatoms and a simultaneous decrease in centric diatoms during the last 200 years, from AD 1876 and onwards.

5.4 Geochemistry

5.4.1 Carbon and nitrogen

The total carbon (TC) and total nitrogen (TN) contents are shown in Fig. 16. TC and TN contents are following the same trends throughout the core, except for in the very top where TC increases, and TN decreases. The highest values of TC content are found in the lowermost samples where it reaches 32 % (AD 1518). Within 17 years (from AD 1518 to 1538) the decrease is drastic and reaches a value of 18 % (AD 1538). Within the same time period, the TN content decreases from 2.3 to 1.5 %. Between AD 1572 and 1645 there are some fluctuations in both TC (between 16 – 21 %) and TN (between 1.3 – 1.6 %). From the late 17th century to the beginning of 19th century the values for both TC and TN content are rather stable (TC around 19 % and TN around 1.5 %) except for one minor peak at AD 1724 (TC around 23 % and TN around 1.7 %). In AD 1803 the values for both TC and TN are again increasing and reaching values of 22 % and 1.6 % respectively. During the rest of the 19th century and the mid 20th century both TC and TN content are fluctuating but the general trend is increasing for both elements until a peak in 1952 where TC is reaching values of 28 % and TN 1.9 %. During the following 18 years the values are drastically decreasing to 18 % for TC and 1.4 % for TN. From 1952 until present there are large fluctuations in both elements. From AD 1952 to 1995 both elements show the same trends but subsequently the elements are fluctuating differently. The last three samples representing AD 2007, 2011 and 2014 show a small decrease in TC (from 26 to 24 %) whereas TN starts to increase already 2004 from 1.73 to 2.14 % This is also seen in the C:N ratio, which decreases during the last years with a, for this record, drastic change from 13.4 in AD 2007 to 11.2 in AD 2014.

As further seen in figure 16 the C:N atomic ratio in the Lake Odensjön sediment sequence ranges between 13 and 17. In the bottom of the core there is a drastic decrease over a 30 year period between AD 1518 and 1548, from 16.1 to 13.6 respectively. After this minimum, it increases again to a value around 15 in the late 16th century. During the 17th century the values were around 15, although with a slow general increase towards the end of the century. In the beginning of the 18th century the trend is again decreasing and values from 16.3 (AD 1708) to 14.7 (AD 1787) were recorded. From AD 1818 to AD 1952 the general trend is increasing from values around 14 to 17, which is the highest value found in the whole record. After this peak at 1952 until the 1970's the ratio is decreasing to 14.7. Hereafter, the C/N ratio is fluctuating until present, and the last sample representing 2014 exhibits the lowest atomic ratio of the whole core (13.09).

5.4.2 Biogenic Silica

The record of biogenic silica content (BSi) is shown in Figure 16. The values are ranging from 28.4 to 55.6 % with generally higher values from the mid-16th century to the mid-19th century. The trends are negatively correlated with TC, with some minor exceptions. The lowermost three samples show relatively low values

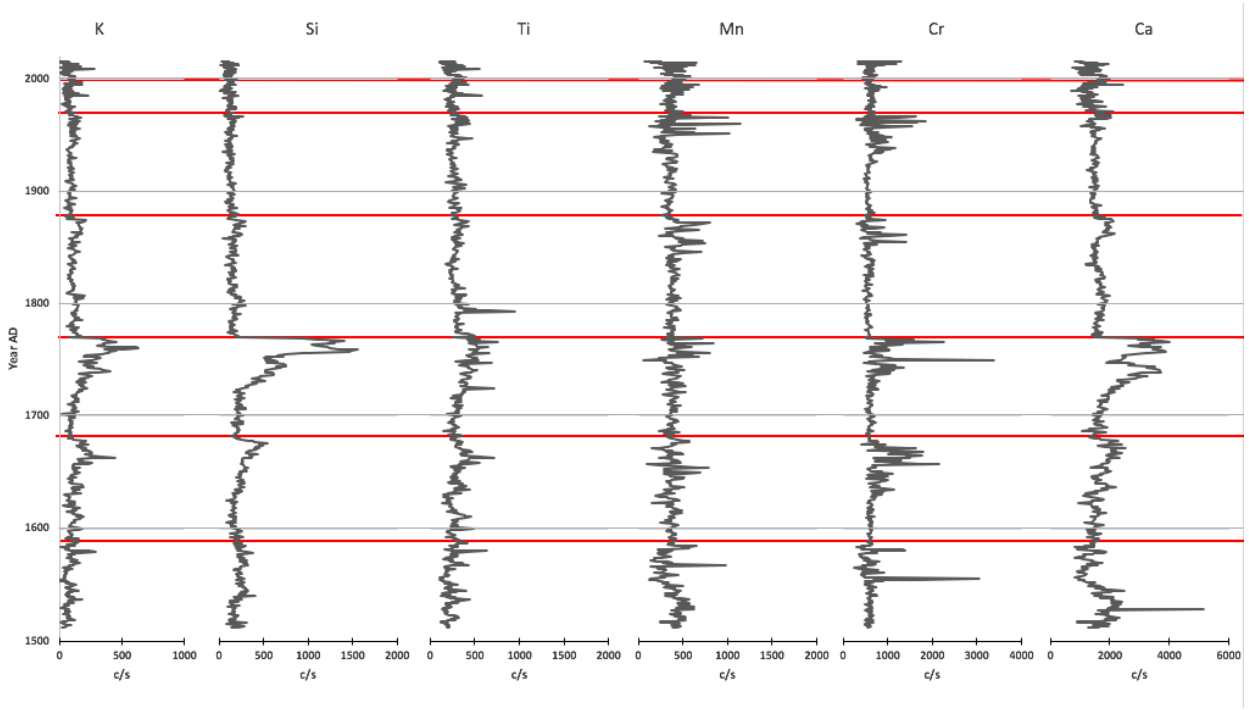

Fig. 17. The XRF results for K, Si, Ti, Mn, Cr and Ca throughout the core. The red lines represent the top boundaries for each sample slab scanned.

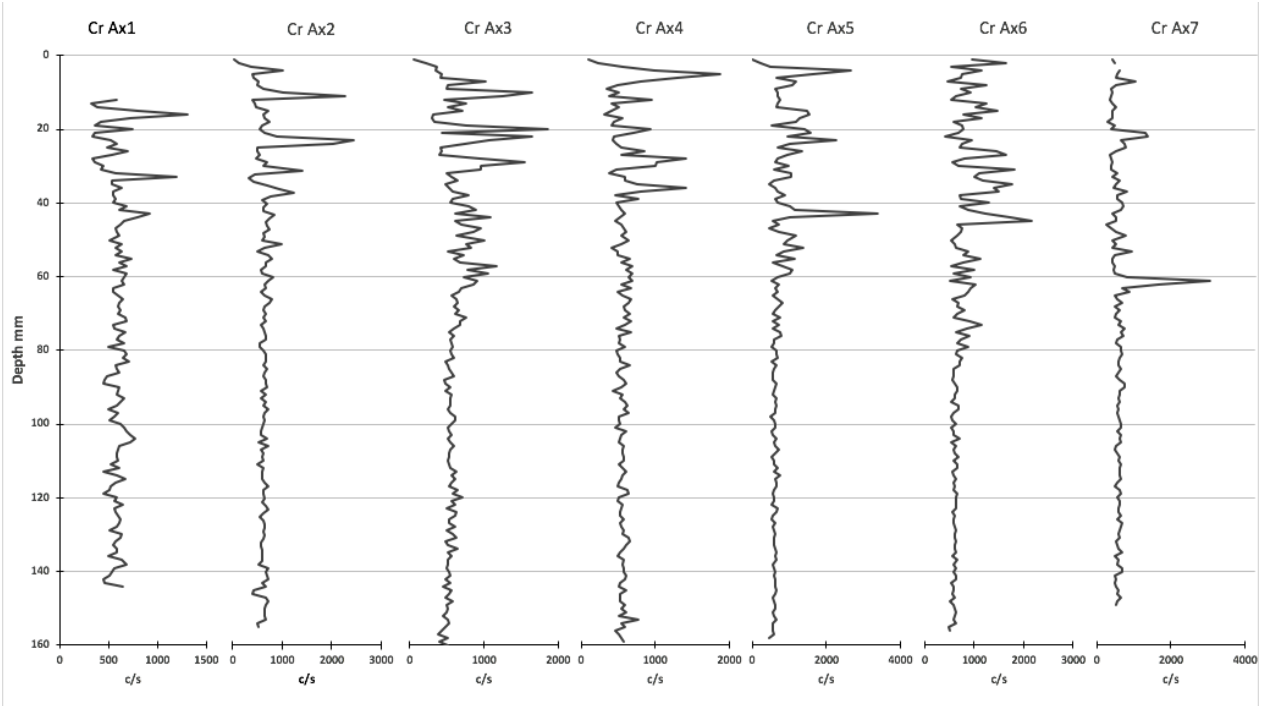

Fig. 18. The distribution of Cr in each sample slab separately where AX1 represents the top of the core. The first mm of AX1 is representing the sediment-water interface therefore the signal starts a few mm down. The analyses are done from top to bottom.

ranging from 28 to 34 %, followed by an increase reaching 55 % within the following 30 years. From this point towards the end of the 17th century BSi content decreases to 47 %, followed by an increase to 55 % within 20 years. The values during the 17th century are relatively stable, ranging from 50 to 55 %. From AD 1692 to 1724 the values decrease drastically from 53 to 41 %. During the 18th century BSi content increases again to values around 50 in AD 1771. The 18th century represents a period of great fluctuations in BSi content. In AD 1803 there is a relatively low value of 45 % followed by a drastic increase to 52 % within 15 years. The next peak with 52 % in AD 1866 is again followed by a drastic decrease to 35 % in AD 1882. The rest of the record until the present shows values around 35 % except for minimum value in AD 1952 at 28 % BSi.

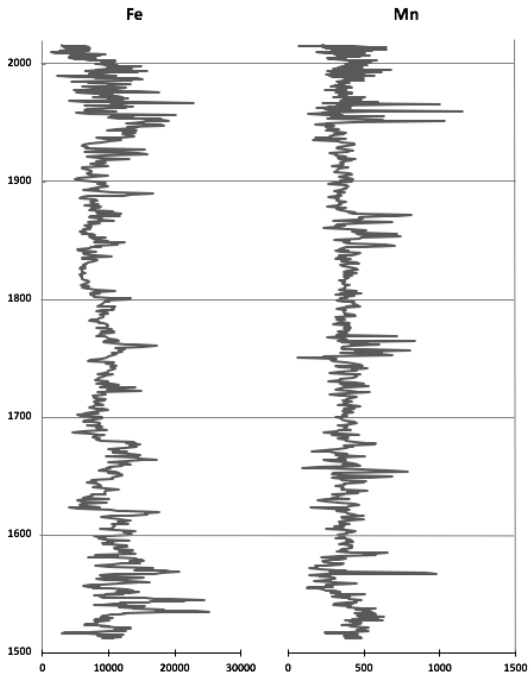

Fig. 19. The distribution of Iron and Manganese throughout the core in c/s.

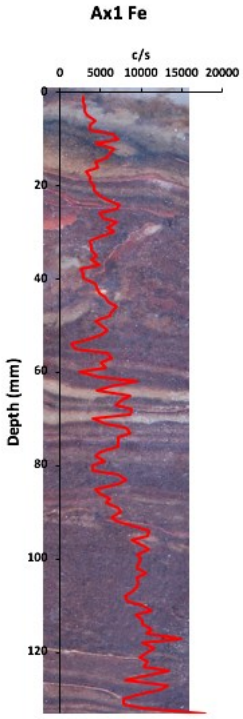

Fig. 20. The Fe record in the uppermost XRF section, representing the top 133 mm of the core. Fe shows higher Fe values in dark laminae than in light. The analysis is done from top to bottom.

5.4.3 XRF analyses

The results of the XRF analysis are interpreted with caution (as further discussed below). Some of the elements (K, Si, Ti, Mn, Cr, Ca) have results that are not considered reliable (Fig. 17). As seen in Figure 17 the values are higher at the beginning of each XRF-scan (they were scanned from top to bottom). This phenomenon is further shown in figure 18. This Figure shows the results for Cr for each individual XRF section. The figure clearly shows that the values are higher in the top of each XRF section and then decrease towards the bottom. AX7, the last XRF section in the core shows a different trend. In this subsection there are not such large peaks as is in the other samples. The higher c/s in the top of the samples is not seen for all elements but for the elements represented in Figure 17. However, some elements are not showing the pattern with a declining trend along the measurement, and these are considered reliable, but still interpreted with caution. For example, as already shown, the Pb record shows a peak during the 1970's which is, as described above, believed to be related to leaded petrol (Fig. 21).

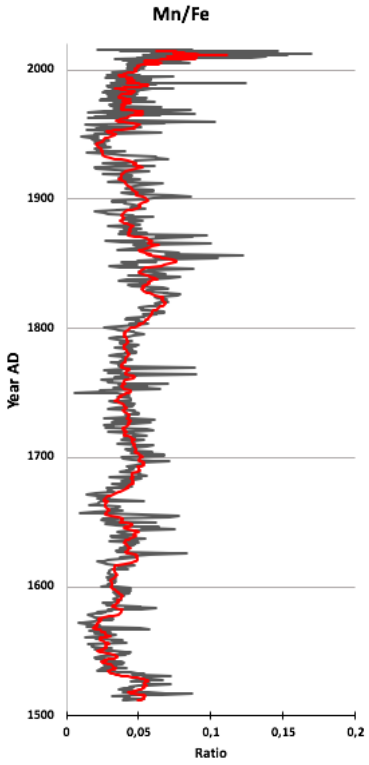

Fig. 21. The Mn/Fe ratio throughout the core. The red line represents a 10 point running average.

5.4.3.1 Iron and Manganese

The Fe record is shown in Figure 19. There are fluctuations in the bottom of the core ranging from 2800 to 25000 c/s with high amplitude peaks. In the middle part of the core, from the end of the 17th century to around 1820 the amplitude of the variations is lower, ranging from 6000 to 17000 c/s. Af-

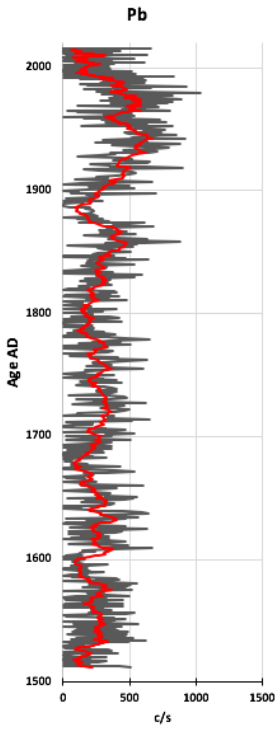

Fig. 22. Pb record. The red line represents a 10 point running average.

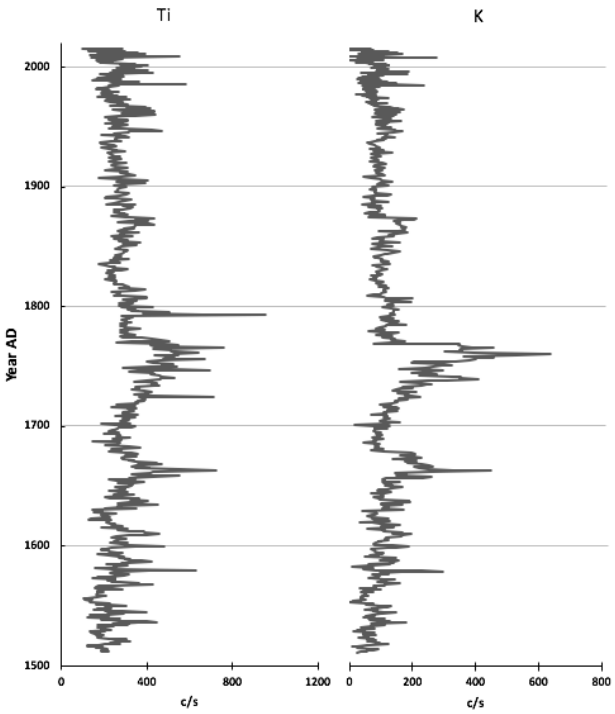

Fig. 22. The distribution of Ti and K throughout the core used for indicator of erosion.

ter AD 1900 until the present the fluctuations are again larger with values ranging from 2200 to 23000 c/s. If the Fe record is studied in more detail, i.e. if the results are put on top of only one sample slab as shown in figure 20. The higher values correspond to the darker laminae whereas lower values correspond to light laminae.

The Mn record is shown in Fig. 19. In the beginning of the record there is a minor increase from around 370 c/s around the beginning of the 16th century and around 600 around AD 1530, followed by a decrease to around 300 c/s around 30 years later. From this point on the values are again increasing to reach around 650 c/s towards the end of the 16th century. The next period of higher amplitude fluctuations is located in the mid 17th century where the values range from 90 to around 700 c/s. The three following periods of high amplitude fluctuation are located around AD 1750, 1850 and 1950, lasting for approximately 30 years each. These higher fluctuations are each situated in the beginning of the XRF sections (see figure 17) and this issue will be discussed further below.

5.4.3.2 Mn/Fe ratio

The Mn/Fe ratio is shown in figure 21. As described above, the Mn values are interpreted with caution due to the higher values in the beginning of each XRF slab, therefore the 10 points running average (hereafter, RPA) is considered here to avoid the high amplitude peaks and further, with the assumption that Fe and Mn have reacted in a similar way during the XRF analysis and that the ratios are not affected even though absolute counts per second changes. In the bottom of the core, from the beginning of the 16th century until the end, the ratio is decreasing from values around 0.05 to 0.009 at around AD 1572. After this, the ratio is slowly increased towards mid 17th century with a ratio around 0.05. After this, the ratio is again decreasing to a ratio around 0.01. During the 18th century the ratio was kept with rather stable around 0.04. In the beginning of the 19th century the ratio is starting to increase from around 0.04 in the beginning of the century to 0.075 around AD 1850. After this

point the general trend is decreasing until around AD 1950 where it reaches a ratio of around 0.02. From that period until the present, ratios are fluctuating largely but with a general increasing trend and the last sample in the record represent a ratio of 0.08.

5.4.3.3 Pb

The Pb record exhibits two periods of elevated values, the first one during the mid 19th century and the second one is divided into two peaks, one during the 1940's and the last one during the 1970's (Fig. 22) After these peaks until the present the Pb values decrease to levels comparable to the bottom of the core.

5.4.3.4 Titanium and Potassium

As for indicators of erosion the fluctuations of K and Ti are used and visualized in figure 23. However, the results were analysed with caution due to the uncertainties with the results from the analysis Both elements show similar trends throughout the core, with large fluctuations in the bottom of the core and a general increase towards a peak during mid 18th century. Here, Ti reaches 760 c/s whereas K peaks at 640 c/s. After this peak, K drastically decreases to values around 130 c/s and remains stable until the mid 19th century where there is a minor increase to values around 215 c/s during the 1870's. For Ti, the values are fluctuating during the period from 1770's to the 1820's, with a slow general decrease. The Ti values are thereafter slowly increasing until the 1860's (reaching 435 c/s) where it is again starting to decrease slightly until 1930's where it reaches 220 c/s. After this period in time, both Ti and K is again showing larger fluctuations towards the top of the core, although not as large as in before 1650's.

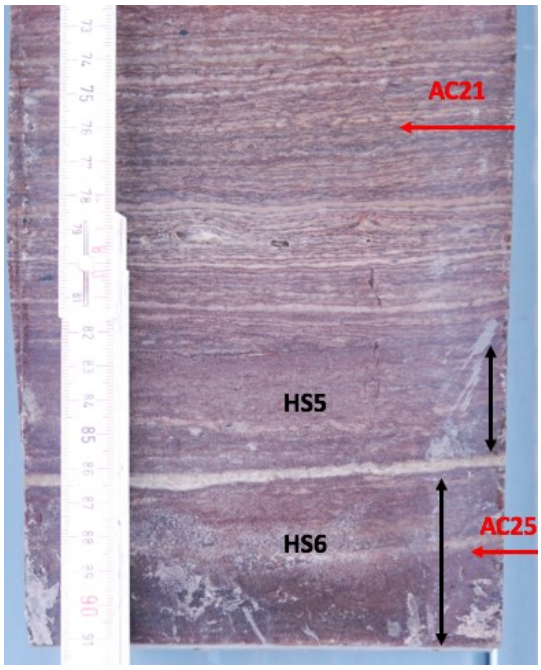

Fig. 24. Figure showing the location of the radiocarbon dates that gave the same age AC21 and AC25. As seen in the picture AC21 was located within laminations and AC25 was located within the undefined section HS6.

6 Discussion

6.1 Chronology

The upper part of the chronology is well constrained by lamina counts and ^{210}Pb. This is shown by the close fit between the lamina counts and the ^{210}Pb dating down to a depth of approximately 270 mm. Below this the lamina and the lead-dates start to diverge, and this is probably due to the characteristics of the sediment. S2 (from 270 to 346 mm of depth) has a darker color and the laminations are harder to distinguish and the possibility of missed laminae is therefore larger. A less probable explanation is that the leaddating gave a slightly too old age but since it fits well with the artificial fall out of ^{137}Cs and ^{241}Am (see figure 8), this is not very likely. When similar sedimentation rates were assumed for the undefined sections (HS1 and HS2) in the upper part of the core (down to a depth of 330 mm) the divergance started earlier (Figure 7). This means, that it is clear that the upper part of the core consists of annually formed varves, and therefore the undefined sections are representing one year of deposition.

Further down the core, there are more undefined sections. HS3 and HS4 (at depths of 425-448 mm and 470-484 mm respectively) these sections are found above all of the radiocarbon dates. This part has the fastest sedimentations rate with an average of 2,36 mm/year.

The radiocarbon analysis was made on large, and well-suited macro fossils for radiocarbon-dating, at depths of 687, 760 and 885 mm, respectively. As seen in Table 3 the result gave ages of 340 ± 40 (AC5) and 430 ± 30 BP (AC21 and AC25). When these ages were calibrated the ages given with the P-sequence were AD 1530, AD 1491 and 1441 AD, respectively. Whereas the counted visible laminae when including the estimates for the undefined sections (i.e where an estimation was made based on sedimentation rate below and above the undefined sections) gave 269, 307 and 404 years (AD 1748, 1710 and 1613, respectively) for the depths of the radiocarbon dates (depths where the macro fossils where found). Consequently, there are "missing" varves and the number of laminae is not matching up to the ages of wiggle matched radiocarbon dates. The most probable explanation for the difference between the number of counted varves and the radiocarbon dates is that visual identification of some lamina was not possible when counting. As the laminae were counted 3 times, it is more likely that some laminae were impossible to distinguish, than laminae being missed or skipped as a result of human counting error. Another possible

explanation is that the radiocarbon dates are too old. However, the sedimentation rates from the laminae counting between these depths and the sedimentation rates from the wiggle matched radio carbon dates are giving similar numbers. The section between 687-885 mm of depth has an average sedimentation rate of 1,8 mm/year if it is calculated with the radiocarbon dates and 2,02 mm/year with the laminae counting. One possible explanation could be that the laminations are not annual. However, that is not very likely due to the fact that there are varves that are formed yearly in the top of the core.

The calibration of the radiocarbon ages was done both wiggle matching (dsequence) and as a stratigraphic model (psequence) in OxCal. For the d-sequence estimations of the number of laminae between the dated horizons were used. Undefined sections (HS5 and HS6, see Table 1 and 3) between the dated levels made the prior input to the wiggle match model uncertain. The model gave an overall agreement index slightly below 60, and low agreement index for the middle sample AC21. Because the gap between the lower and upper dates fits well it is likely that AC21 is too old. There are a few alternative explanations for the erroneous age. Either, there has been fast sedimentation in the bottom part of the core and the two bottom radiocarbon samples have been deposited close in time. As there are undefined sections in the bottom of the core this could be a possibility. However, the AC21 was found within the laminated part of the core and AC25 was found in an undefined section (HS6). Therefore, the exact number of laminae between these two samples is not known and the number of laminae used as prior in the model was based on an estimate done by comparing the number of laminae above and below the undefined sections. The last radiocarbon date, AC25 was taken within an undefined section (HS6) and above this, HS5 is situated (see figure 24). This means that the closest set of laminations that could be used for the estimation of sedimentation rate is situated 50 mm above the radiocarbon date and there are no laminations to compare with below this radiocarbon date (AC25). Another possibility is that the macro-fossils have been redeposited or moved while coring. If the sample has been moved while coring (i.e. moved within the stratigraphy), even if that is not likely, the only possible sample is AC25 because that sample was not found within laminae whereas the other two samples were found in-between laminae.

However, AC25 was found within the sediment in a way that makes moving of material while coring unlikely. Another possibility is that there was a redeposition of the macro-fossil in the catchment. However, there are at least 53 visible and counted laminae between these samples (AC21 and AC25), in this case, the macro-fossil should have been kept in the catchment for at least 53 years before redeposition.

The result from the P-sequence was used to construct the age-depth. The P-sequence was preferred over the Dsequence due to the uncertainties of the number of laminae between the radiocarbon-dates. Moreover, the Psequence was used because the prior used in this model is less strict than the priors used in D-sequence where more details are put into the model.

6.2 Geochemistry

6.2.1 XRF

Initially, the purpose of the XRF analyses was to be able to have a 0.1 mm resolution on the results to be able to reconstruct variations on varve-scale, and use the elemental composition for counting varves. To limit the analysis time and the thawing of the subsamples, the count time on each step was kept short. This resulted in low counts, sometimes below detection limit and high noise levels. To increase the signal 10 sepctra were summed, and the results are presented with 1 mm resolution. Therefore, some of the information on laminae was lost due to the fact that some of the laminae were thinner than 1 mm, and the variations within the laminations could not be analyzed.

The results from the XRF scan have features that indicate problems with the analysis and some of the results are interpreted as unreliable. The results were probably affected by the methods used during the analysis. As described above and seen in Figure 17, there are higher c/s of these elements in the top of every scanned XRF section. The samples were scanned from top to bottom once, and the beginning of the graphs represents the top of each sample (as in figure 17 and 18). One possible effect on the result is that frost and water accumulated on the surface of the frozen sample during scanning. Since each sample took about one hour to scan, the surface was first covered in frost and with time, the surface started to thaw and created an additional water film between the sample surface and the plastic film. This effect probably contributed to the lower counts at the end of the scans. The sediment sections also shrunk while thawing, increasing the distance from the scanner, also contributing to lower counts. The samples were only scanned once from top to bottom. This effect could possibly have been avoided by letting the samples thaw on the surface before scanning to ensure that the results reflected similar conditions on the surface, and use longer scan times to increase the signal. There was however concerns that the high water content in the uppermost samples of the core would make the sample melt too much during an hour of analysis.

When Gregory et al. (2018) tested a method for running XRF-scans on frozen sediment samples, they used a well-insulated containment vessel with double Styrofoam walls. The walls were separated by high-density polyethylene sheets that were filled with freeze pack gel to prevent thawing while scanning. Before their analyses they kept the sample in room temperature for half an hour to ensure that the plastic film was adhered to the sediment surface. In contrast, when the analyses for this thesis were measured, the samples were kept in Styrofoam boxes with no further isolation or freeze pack gel. The plastic film was put on the sediment as soon as it was taken out of the freezer. Gregory et al. (2018) reported an increase in c/s in the end of the analysis of each sediment slab which is in contrast to my results where the higher c/s was found in the top or the beginning of each scan. Gregory et al. (2018)

rejected the hypothesis that the increase was caused by a thin water film created on the surface of the sediment while it was thawing. They could reject this effect due to the lack of gradual increase in X-ray scatter during scanning, which was not observed in their study. Moreover, they scanned multiple cores with varying length and observed the same effect, suggesting that this could not be due to the melting of the core material. Further, Gregory et al (2018) could reject the effect of condensation and therefore an increased distance between the sediment surface and the plastic film, by an examination of the Ar record that showed no obvious increase coeval with a rapid increase in X-ray scatter. However, Gregory et al (2018) suggest that the analyses should be done under low humidity conditions to minimize the risk of condensation. Preferably during the drier winter months. Gregory et al (2018) also point out the importance of a smooth and even surface of the sediment. To minimize the error the researchers further scanned each sample from top to bottom and vice versa. My analyses were only done from top to bottom once. As shown in Figure 17 and 18 the increased c/s is in the top part of the samples, after approximately one third of the sample the c/s starts to decrease more or less gradually to more stable values, with less high amplitude peaks. This might be explained by the fact that the frost on the surface was thawed after one third of the analysis (20 minutes) or maybe that the surface of the sediment was also thawing, and this affected the results from the XRF. This effect should have been further evaluated by scanning the samples from both directions or to thaw the surface of the sediment before analysis.

The organic matter content of the sediment can also influence the XRF measurements. The signal emitted from the sediment sample surface to the X-ray fluorescence detector is a function of the composition of the sediment. The light elements such as C, O and N that form a large part of organic matter are outside the range of measuring on the XRF-detector (Löwemark et al. 2011). As these elements are diluting the effect it is resulting in lower counts per second for the heavier elements i.e. higher organic matter content results in lower counts detected for all the detected elements (Calvert, 1983: Rollinson, 1993). The results from the XRF analyses for this project were initially given in a 0.1 mm step size resolution and thereafter added up to 1 mm. This was done because the low signal and very noisy result. This could have been caused by the high organic content in the sediment. Furthermore, my analyses were performed with a 2 sec exposure time and according to Cuven et al. (2015) the exposure time can also have an effect on the results. Cuven et al. (2015) tested different exposure times on different types on sediment to determine the best settings for obtaining good results (less noise) and recommended 10-20 seconds exposure time for lacustrine sediments high in organic matter. As my analyses where performed with an exposure time of 2 seconds, this might have caused the low c/s obtained and noisy results. Löwmark et al. (2011) further investigated if and to what extent Al measured by the XRF-scanner could be used to normalize other elements and by this reach better assessments of their relative change in organic rich sediments. They found that the elements and their measurements from the XRF detector were strongly influenced by the organic components of the sediments, and reached the conclusion that the signals should be normalized against a conservative element or a standard. They further found that Al was the most suitable element for normalizing due to the fact that Al is little affected by redox and biological processes. My results from both the smear-slide analysis and bulk C and N analysis show that the sediment has a rather high content of organic material and carbon. However, even if Al is used for normalization of the other elements, the increased c/s in the uppermost part of each sediment slab cannot be corrected for. Furthermore, Löwemark et al (2011) points out that the poor detection limits for Al, the sediments should be measured with different X-ray tubes to obtain the full spectrum of the element whereas my analyses were only preformed once, with a Rh tube. As the studied literature provides no conclusive explanation of the higher amplitude peaks in the beginning of the sediment slaps that are seen in this study (igure 17), the conclusion drawn from the results from this thesis is that this is a result of the thawing sediment, as no other plausible factors was identified which could have caused such results.

6.2.2 Pb

There is an increase in Pb around AD 1530 (see figure 22) that might reflect the increased silver ore processing in continental Europe at this time that used lead in the process of extracting silver (Brännvall et al. 2001). Furthermore, a decrease is seen after AD 1648 which Brännvall et al. (2001) attribute to the Thirty Years War (AD 1618-1648). The major increase in lead in the sediment is starting in the beginning of the 20th century which is in agreement with what Renberg et al. (2000) have seen in their study. Furthermore Brännvall et al. (2001) point out that, even if the industrial revolution started already in the mid 19th century it is not until the 20th century we can see a large increase in the lead pollution. In my results there are three periods of higher values during the 1930's, 1940's and 1970's. The peak in the 1930's is also seen in the study by Renberg et al. (2000) as they found a minor increase in the $^{206}Pb/^{207}Pb$ ratio at this time in Lake Nylandssjön in the north of Sweden. However, they are not further explaining the reason for this minor increase. The second peak, during the 1940's is reflecting the increase in the use of lead after the Second World War and the last one the added lead in the gasoline and the prohibiting thereof that caused the decrease after the 1970's (Brännvall et al. 2001; Smol, 2008).

6.3 C:N and BSi and the development in and around Lake Odensjön

6.3.1 1500 – 1800 AD

As mentioned in the introduction, at this time the crown owned the mature forest and the farmers were only allowed to use *Alnus*, *Betula*, *Salix* and *Corylus* that was growing on the wetlands and it was not until the end of this period that the deforestation started. What happened at this time in the direct vicinity of

Lake Odensjön have not been found in the literature. However, there is an ecological response to changes in the environment found in the lake record described below.

C:N ratios are used as an indicator of the relative contribution of terrestrial and aquatic organic matter in a lake system. Ratios below 10 indicate dominance of algal organic matter whereas ratios above 20 indicate high proportion of terrestrial organic matter (Meyers, 1994) The C:N ratios in the core have values ranging from 11.2 to 14.6. In the lower part of the core the ratio starts with three rather high values (for this core) around 13 in the end of the 15th century to the beginning of 16th century. After this there is a drastic decrease from almost 14 to 11.6 within 30 years. The reason for this drastic change is unclear but a similar, and reverse trend is seen in the BSi and it might imply a change in the algae community, where the diatoms are outcompeting other primary producers. However, a cold phase lasting from AD 1440-1470 has been described by Zawiska et al (2017). They used Chironomidaebased transfer functions and assemblages of Chironomidae fossils in the lake sediments of Atnsjøn in the south of Norway. The results showed a colder period during this time. This cold period was coinciding with a pronounced negative NAO phase (Trouet el al. 2009) and a large volcanic eruption in AD 1452 at Kuwae Island in Vanuatu, the climate effects of this eruption have been described worldwide (Witter and Self, 2006). Though, this period was not included in my record, the drastic change in the beginning of the record might be a response to the climate change at this time. However, this is only a speculation of what could have caused the drastic change in the beginning of the record. Even if the answer to the change cannot be found here, the change in both C:N and BSi is indicating an ecological change in the environment around the lake at this time.

After this drastic decrease in C:N the ratio starts to increase again from 1550's and is increasing until the beginning of the 1700's. Again, the BSi is reacting in a similar but reverse trend except for one shift in the beginning of the 1600's. At this depth, from 670 to 690 mm (AD 1613 to 1598) there are two thick light laminae. This also coincides with the second highest number of counted diatoms from the smear-slide analysis (sample from 662 mm of depth, Figure 15). This sample was taken from a thick light lamina and was therefore easy to sample and be sure that the sample was taken from one lamina only. Therefore, the result might be regarded as a bit biased though the second highest number of diatoms were found in a sample taken from a thick light layer. It could be suspected to contain a high number of diatoms. This might not say, though that the BSi is highest at this depth however, it is an increase in the BSi in the beginning of 17th century. And this tells us that there is a large number of diatoms in the sampled layer, both from results from smearslides and BSi. The color of the sediment also changes at this depth, from a darker brown to a more reddish brown. The change in color coincides with an increase in the Fe c/s that starts around AD 1622 (Figure 20). Further this is also where there is a shift from a dominance of pennate diatoms to a dominance of centric diatoms at 662 mm of depth, corresponding to around AD 1619 (Figure 14). The centric diatoms are dominating until around AD 1815 where it is shifting again, and the pennate diatoms are again dominating towards the present. The majority of centric diatoms are planktonic (Cohen, 2003). There might have been an environmental change in the lake system at this time that was more favorable for one group of diatoms. One possible effect is the land-use changes in the beginning of the 19th century when the deforestation started that might have changed the environment in the lake to more favorable conditions for the pennate diatoms. If the taxonomy of the diatoms had been studied further, questions regarding their environment and the changes within the lake system could have been answered. The diatom community within a surface water is controlled by a range of factors such as temperature, pH, nutrients and they respond rapidly to environmental changes (Battarbee, 1991) So if the full diatom distribution is studied, the changes in species composition could have been used to answer more details about the environment in the lake, but it was outside of the scope of this project.

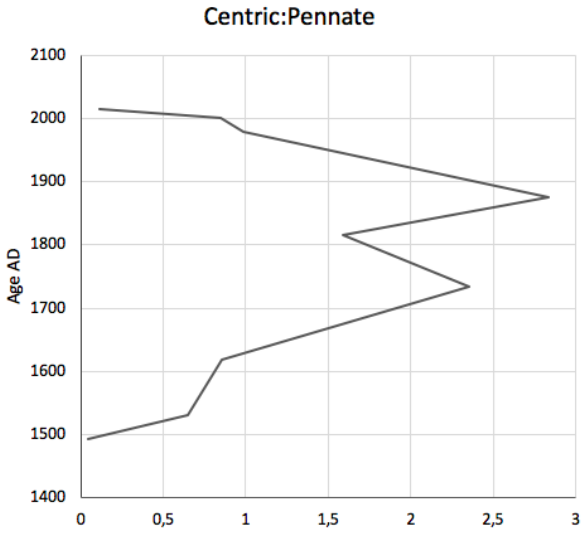

Fig. 25. Centric:Pennate ratio and how it is changing throughout the core.

6.3.2 1800 - 1950 AD

The influx of terrestrial inorganic and organic matter to a lake is affected by the catchment erosion and the processes taking place within the environment, such as land use, human activities, precipitation and vegetation cover (Engstrom and Wright, 1984) It seems like the C:N ratio in Lake Odensjön has been affected by the landuse change in the beginning of the 19th century. At the time for forest clearing on Söderåsen the C:N ratio starts to increase (see figure 16). In approximately 130 years the C:N ratio increases from 12 to 14. Even if this change in ratio is small, it is coinciding with the time of deforestation and this might have led to an increase in transport of terrestrial material to the lake but the primary producers were still a large contribution to the organic material in the lake. Kaushal and Binford (1999) found a higher proportion of terrestrial organic matter and an increase in the C:N ratio following the deforestation caused by the European settle-

ment within the catchment area of Lake Pleasant in Massachusetts, USA. However, the increase in that lake system was larger than the change in Odensjön as a result of deforestation. One possible explanation for this is that lake Odensjön and its catchment is very small and the effect of land use change might not have had a significant consequence for the lake system in terms of changes in C:N ratio. Moreover, the deforestation might not have been so large immediately around the lake because of the talus slopes surrounding the lake. However, there is a large difference between S1 and S2 in the leaf content and the boundary is very sharp so there must at least have been a change in the vegetation cover surrounding the lake at this point in time, around AD 1930. Furthermore, even if the Ti results from the XRF is being analyzed with caution there is a minor increase in Ti at the beginning of the 18th century that might imply increase in erosion at this time. However, this coincides with the elevated c/s in the beginning of AX4 slab and it can therefore not be regarded as a reliable proxy for erosion. Furthermore, if the environment around the lake is taken into consideration in this analysis it might be hard to distinguish changes in erosion due to deforestation. The lake is surrounded by talus slopes and the direct vicinity of the lake might not have been changed so drastically during deforestation since it was considered as "unusable land". Therefore, the change in erosion might not be seen in the results in a great extent. The abrupt change in color between S2 and S3 is coinciding with the time period when Söderåsen was as most open and the deforestation was largest around AD 1850. Except for one exception in the BSi at AD 1866 with 51.8 % there is a general decrease in BSi from the beginning towards the end of 19th century. The decrease from that outlier to 34 % at AD 1882 coincides with the change in characteristics of the sediment. The darker part, S2 has its onset around AD 1869 and lasts until 1952 when the concentrations of leaves were high in the sediment. The increase in C:N ratios however, started already in the beginning of the 19th century and the increase lasted until AD 1952. Something changed in the environment in the lake at the onset of the deforestation in the area. The BSi decreased while the C:N ratios increased. The diatom community was probably facing environmental changes that were not favorable for them as a consequence of deforestation. Diatom concentrations were also lower from the beginning of the 19th century until the present. There was also a change in the morphological groups of diatoms at these depths (see figure 14). At the depth of 662 mm (AD 1619, see figure 25), the community changes from being dominated by pennate diatoms to centric diatoms. The centric:pennate ratio can be used in estuarine systems as an indicator of loss of benthic habitat (pennate is often benthic) and nutrient enrichment (Stoermer and Smol, 2001). If therefore, the increase in pennate corresponding to the decrease in centric means nutrient enrichment this would have taken place from the 17th century towards the end of 19th century. This cannot be explained by the deforestation only. Therefore, there might have been another nutrient load that have entered the lake in an earlier stage as the shift from pennate to centric domination starts already around AD 1530, at depths of around 800 mm (see figure 14).

6.3.3 1950 AD - today

The uppermost part of the core is represented by the last 67 years and most of the S1 section of the sediment. Here it has been demonstrated that there are annually formed laminations. The C:N ratio is generally decreasing towards a lower ratio than was seen as a response to the deforestation. The high abundance of leaves is not seen in the results as expected, as a high abundance of leaves would result in a higher C:N ratio. The ratio was expected to be higher here since the sediments have a high abundance of *Fagus* leaves. The C:N ratio is also showing greater variability during the last couple of years ranging from 11.8 to 13.4, which might indicate differences in leaf content of the samples. The BSi is increasing with 10 % units from AD 1952 to 1963 but after this point the BSi is stable until today with a value around 36 %.

6.4 Mn/Fe ratios

Mn/Fe ratios have been repeatedly used as an indicator of redox conditions in lakes (Wersin et al. 1991; Loizeau et al. 2001; Koinig et al. 2003; Dean & Doner, 2012). In all these studies lower Mn/Fe ratios are interpreted as lower O2 concentrations in the water column and vice versa.

Interestingly, the Mn/Fe ratios (even if it is interpreted with caution due to the XRF results, especially regarding Mn) follow the same general pattern throughout the core as the BSi and TC, with high Mn/Fe during periods with high BSi and low TC. Furthermore, even if the smearslide analyses were semiquantitative and do not represent true concentrations, a shift from pennate to centric could mean an increase in nutrient load to the lake system and that the amount of oxygen in the water column is a limiting factor for the diatom community as a whole including both centric and pennate diatoms. This might imply that the lake system and the ecology within it are sensitive to changes in the nutrient load transported to the lake.

7 Conclusions

- The sediment sequence from Lake Odensjön consists of annually laminated sediments, at least in the uppermost part of the core (down to a depth of 330 mm) •
- **The varves are of biologic origin consisting of both autochthonous and allochthonous material from the lake and its catchment.**
- **The determination of the age of the sediment was done using ^{210}Pb dating, radiocarbon dating and lamina counting. The results of these three methods suggest that the sediment sequence is representing the time frame from around 1450 AD until present. The lowermost radiocarbon date gave the result of 430 ± 30 years before present. However, cautions have to be made because two**

lowermost radiocarbon dates gave the same age and due to the uncertainty of the counted laminae between these two dates the P sequence (that only uses depth as prior) was used for wiggle matching. If the laminae between these two radiocarbon dates had been more precise, the D sequence could have been used to get a more precise age-depth model.

- Changes in the environment indicated by the analysis BSi, C:N and smearslides the sediment itself. There are changes in colour and the thickness of the laminations throughout the core. The largest change was likely caused by deforestation in the 19th century. From around AD 1860 the characteristics of the sediments changed and there was a change in dominating morphological diatom group. The C:N increased at the same time as the deforestation as a consequence of increased deposition of terrestrial organic matter. However, the BSi content did not respond in the same manner as the C:N. The BSi content responded to the change when landscape openness reached a maximum.

- The problems encountered with the unreliable XRF data is showing higher values (counts) in the uppermost part of each analyzed sample could possibly be avoided by using the methodology suggested by Gregory et al. (2018). They used a double insulated box to store the core or sediment slabs during analysis. Moreover, they thawed the surface of the sample before analysis to avoid the effects of thawing during analysis.

- To ensure reliable XRF results one suggestion for the future is to have a longer exposure time for a sediment with high organic matter content. However, this can be hard to do on frozen samples with high water content. Therefore, I suggest that the XRF analysis might be better to perform on samples stored in better insulated boxes to ensure that the samples are kept frozen during the whole analysis.

- For future studies on this sediment and the evolution of the lake and the local and regional environment over time. One suggestions is to identify the taxa to species or even genera level, in addition to the centric-pennate ratio used here. This could help to further analyze and answer the questions in this project.

8 Acknowledgements

During the process of writing this thesis many people have contributed with their time, knowledge and effort. First of all, special thanks are given to my supervisors Karl Ljung and Dan Hammarlund. You have given me valuable inputs and I have enjoyed the discussions and the knowledge you have shared along the process. Another special thanks to Carla Nantke for walking me through the process of Biogenic Silica analysis. Further, I want to thank Marie-Louise Siggaard-Andersen at Centre of GeoGenetics at the Natural History Museum of Denmark for your shared knowledge during the process of XRF analysis and the interpretation of the results.

Thanks to David for your endless support and for what you are giving me. Last but not least, many great thanks to the Department of Geology in Lund and the ambitious professors and teachers. I have enjoyed every step pf my five years of education here.

8 References

Appelby, P. G. 2001: Chronostratigraphy techniques in recent sediment. In W:M Last and J.P Smol (eds) *Tracking Environmental Change Using Lake Sediments*. Vol 1: *Basin Analysis Coring, and Chonrological Techniques*. Dordrecht: Kluwer, 171-203

Appelby, P. G. & Oldfield, F. 1978. The calculation of ^{210}Pb dates assuming a constat rate of supply of unsupported ^{210}Pb to the sediment. *Catena 5*, 1-8.

Battarbee, R.W. 1991. Paleolimnology and climate change. In Frenzel, B., editor; *Evaluation of climate proxy data in relation to the European Holocene.* Akademie der Wissenschaften under der Litteratur Mainz, 149-157.

Berglund, B. E. & Rapp, Anders. 1988: Geomorpholo gy, climate and vegetation in north-west Scania, Sweden, During the late Weichselian. *Geographia Polonica 55*, 13-35

Bonnizzoni, L., Maloni, A., Milazzo, M. 2014. Evalu ation of effects of irregular shape on quantita tive XRF analysis of metal objects. *X-ray Spectrometry 35*, 390399

Brauer, A. 2004. Annually laminated lake sediments and their paleoclimatic relevance. In: Fisher H., Kumke, T., Lohmann G and et al. (eds) *The Climate in Historical Times: Towards a Synthesis of Holocene Proxy Data and Climate Models* (GKSS Scool of Environmental Research) Berlin: Springer-Verlag. 111-129.

Brännvall, M. L., Bindler, R., Emteryd, O., Renberg, I. 2001. Four thousand years of atmospheric lead pollution in Northern Europe: A summary from Swedish lake

Sediments. *Journal of Paleolimnology 25*. 421-435.

Böning, P., Bard, E., Rose, J. 2007 Toward direct, micron-scale XRF elemental maps and quantitative profiles of wet marine sediments. *Geochemistry, Geophysics, Geosystems 8:5.* 1-14.

Calvert, S.E. 1983 Geochemistry of Pleistocene sapropels and associated sediments from the east-

ern *Mediterranean. Oceanologica Acta 6*, 255267.

Cambray, R.S., Playford, K., Lewis, G. N. J., Carpenter, R.C., and Gibson, J.A.B. 1987. Observations on radioactivity from Chernobyl accident. *Nuclear Energy* 26 77101.

Cohen, A. S. 2003. *Paleolimnology the history and evolution of lake systems*. New York: Oxford University Press. 1-525.

Conley D. J. 1998: An interlaboratory comparison for the measurement of biogenic silica in sediments. *Marine Chemistry 63*, 39-48.

Croudace, I. W., Rothwell, R. G. (Eds) 2015. *Micro-XRF studies of sediment cores. Applications of a non-destructive tool for the environmental sciences.* Developments in Paleoenvironmental Research. Dordrecht: Springer. 1-656.

Cuven S., Francus P., Crémer J, F., Bérubé F. 2015. Optimization of Itrax Core Scanner Protocols for the Micro X-Ray Fluorescence Analysis of Finely Laminated Sediment: A Case Study of Lacustrine Varved Sediment from the High Arctic. In Croudace I, W. and Rothwell R, G (eds). *Micro XRF Studies of Sediment Cores. Application of a non-destructive tool for the environmental sciences.* Dordrecht. Springer, 1 - 668.

Dean, W. & Doner, L. 2012. A Holocene record of endogenic iron and manganese precipitation and vegetation history in a lake-fen complex in northwestern Minnesota. *Journal of Paleolimnology 47,* 29-42.

DeMaster D. J. 1981: The supply and accumulation of silica in the marine environment. *Geochimica en Cosmochimica Acta 45*, 1715-1732.

Eggimann D. W., Manheim F. T., Betzer P. R. 1980: Dissolution and analysis of amorphous silica in marine sediment. *Journal of sedimentary petrology 50*, 215225.

Engstrom D, R. and Wright H, E, J. 1984. Chemical stratification of lake sediments as a record of environmental change. In Haworth E, Y. and Lund J.W.G (Eds) *Lake sediments and Environmental History.* Leicester University Press, Bath. 11-68.

Geil, E. C. & Thorne, R. E. 2014 Correcting for surface topography in X-ray fluorescence imaging. *Jornal of Synchotron Radiation, 21:6*, 1358-1363.

Gregory, B.R.B., Patterson, R.T., Reinhardt, E.G., Galloway, J.M. 2018. The iBox-FC: A new containment vessel for Itrax X-ray fluorescence core-scanning of freeze cores. *Quaternary International.* https://doi.org/10.1016/.quaint.2018.09.008.

Hardy, E.P. 1977. Final tabulation of monthly 90Sr fallout data, 1954-1976. *Envir.* Quat. HASL 329, U.S. Dept. Energy, New York.

Håkansson, T. 1948. Skogslandskapets historia under 300 år i Konga socken i Skåne. *Svenska Skogsvårdsföreningens Tidskrift 4.* 239-264.

Kausal, S., & Binford M.W. 1999. Relationship between C:N ratios of lake sediments, organic matter sources, and historical deforestation in Lake Pleasant, Massachusetts, USA. *Journal of Paleolimnology 22*, 439-442.

Koinig, K. A., Shotyk, W., Lotter, A.F., Ohlendorf, C., Sturm, M. 2003. 9000 years of geochemical evolution of lithogenic major and trace elements in the sediment of an alpine lake – the role of climate, vegetation and land-use history. *Journal of Paleolimnology 30*, 307-320

Lantmäteriet, 2018. Historical maps. Search details: Odengården, Röstånga, Nackarp, Solbacken, Torpet i Röstånga, Skåne län. https:// historiskakartor.lantmateriet.se/historiskakartor/searchresult.html?archive= GEOIN&firstMatchToReturnLMS=1&firstMatchToReturnREG=1&firstMatchToReturnRAK=1&yMin=6206871&xMin=391466&yMax=6208871&xMax=393466&locale=en_ US Received: 20180912

Loizeau, J.L., Span, D., Coppee, V., Dominik, J. 2001. Evolition of the trophic state of Lake Annecy (eastern France) since the last glaciation as indicated by iron, manganese and phosphorus specation. *Jounal of Paleolimnology 25*, 205-214.

Meyers P.A. 1994. Preservation of elemental and isotopic source identification of sedimentary organic matter. *Chemical Geology 114,* 289-302.

Meyers P. A., Leenheer M J., Eadie B J., Maule S J. 1984: Organic geochemistry of suspended and settling particulate matter in Lake Michigan. *Geochimica et Cosmochimica Acta 48,* 442-452.

Nealson, K. H. Saffarini, D. 1994: Iron and manganese in anaerobic respiration – environmental significance, physiology and regulation. *Annual Review of Microbiology 48*, 311-343

O'Sullivan P. E., Reynolds, C.S., 2005: The Lakes Handbook: Lake Restoration and rehabilitation. Blackwell Science, Oxford.

Ojala, A.E.K., Francus, O., Zolitschka B., et al. 2012.

Tidigare skrifter i serien ”Examensarbeten i Geologi vid Lunds universitet”:

557. Nilsson, Hanna, 2019: Records of environmental change and sedimentation processes over the last century in a Baltic coastal inlet. (45 hp)
558. Ingered, Mimmi, 2019: Zircon U-Pb constraints on the timing of Sveconorwegian migmatite formation in the Western and Median Segments of the Idefjorden terrane, SW Sweden. (45 hp)
559. Hjorth, Ingeborg, 2019: Paleomagnetisk undersökning av vulkanen Rangitoto, Nya Zeeland, för att bestämma dess utbrottshistoria. (15 hp)
560. Westberg, Märta, 2019: Enigmatic wormlike fossils from the Silurian Waukesha Lagerstätte, Wisconsin, USA. (15 hp)
561. Björn, Julia, 2019: Undersökning av påverkan på hydraulisk konduktivitet i förorenat område efter in situ-saneringsförsök. (15 hp)
562. Faraj, Haider, 2019: Tolkning av georadarprofiler över grundvattenmagasinet Verveln - Gullringen i Kalmar län. (15 hp)
563. Bjermo, Tim, 2019: Eoliska avlagringar och vindriktningar under holocen i och kring Store Mosse, södra Sverige. (15 hp)
564. Langkjaer, Henrik, 2019: Analys av Östergötlands kommande grundvattenresurser ur ett klimtperspektiv - med fokus på förstärkt grundvattenbildning. (15 hp)
565. Johansson, Marcus, 2019: Hur öppet var landskapet i södra Sverige under Atlantisk tid? (15 hp)
566. Molin, Emmy, 2019: Litologi, sedimentologi och kolisotopstratigrafi över krita–paleogen-gränsintervallet i borrningen Limhamn-2018. (15 hp)
567. Schroeder, Mimmi, 2019: The history of European hemp cultivation. (15 hp)
568. Damber, Maja, 2019: Granens invandring i sydvästa Sverige, belyst genom pollenanalys från Skottenesjön. (15 hp)
569. Lundgren Sassner, Lykke, 2019: Strandmorfologi, stranderosion och stranddeposition, med en fallstudie på Tylösand sandstrand, Halland. (15 hp)
570. Greiff, Johannes, 2019: Mesozoiska konglomerat och Skånes tektoniska utveckling. (15 hp)
571. Persson, Eric, 2019: An Enigmatic Cerapodian Dentary from the Cretaceous of southern Sweden. (15 hp)
572. Aldenius, Erik, 2019: Subsurface characterization of the Lund Sandstone – 3D model of the sandstone reservoir and evaluation of the geoenergy storage potential, SW Skåne, South Sweden. (45 hp)
573. Juliusson, Oscar, 2019: Impacts of subglacial processes on underlying bedrock. (15 hp)
574. Sartell, Anna, 2019: Metamorphic paragenesis and P-T conditions in garnet amphibolite from the Median Segment of the Idefjorden Terrane, Lilla Edet. (15 hp)
575. Végvári, Fanni, 2019: Vulkanisk inverkan på klimatet och atmorsfärcirkulationen: En litterarurstudie som jämför vulkanism på låg respektive hög latitud. (15 hp)
576. Gustafsson, Jon, 2019: Petrology of platinum-group element mineralization in the Koillismaa intrusion, Finland. (45 hp)
577. Wahlquist, Per, 2019: Undersökning av mindre förkastningar för vattenuttag i sedimentärt berg kring Kingelstad och Tjutebro. (15 hp)
578. Gaitan Valencia, Camilo Esteban, 2019: Unravelling the timing and distribution of Paleoproterozoic dyke swarms in the eastern Kaapvaal Craton, South Africa. (45 hp)
579. Eggert, David, 2019: Using Very-Low-Frequency Electromagnetics (VLF-EM) for geophysical exploration at the Albertine Graben, Uganda - A new CAD approach for 3D data blending. (45 hp)
580. Plan, Anders, 2020: Resolving temporal links between the Högberget granite and the Wigström tungsten skarn deposit in Bergslagen (Sweden) using trace elements and U-Pb LA-ICPMS on complex zircons. (45 hp)
581. Pilser, Hannes, 2020: A geophysical survey in the Chocaya Basin in the central Valley of Cochabamba, Bolivia, using ERT and TEM. (45 hp)
582. Leopardi, Dino, 2020: Temporal and genetical constraints of the Cu-Co Vena-Dampetorp deposit, Bergslagen, Sweden. (45 hp)
583. Lagerstam Lorien, Clarence, 2020: Neck mobility versus mode of locomotion – in what way did neck length affect swimming performance among Mesozoic plesiosaurs (Reptilia, Sauropterygia)? (45 hp)
584. Davies, James, 2020: Geochronology of gneisses adjacent to the Mylonite Zone in southwestern Sweden: evidence of a tectonic window? (45 hp)
585. Foyn, Alex, 2020: Foreland evolution of Blåisen, Norway, over the course of an ablation season. (45 hp)
586. van Wees, Roos, 2020: Combining luminescence dating and sedimentary analysis to derive the landscape dynamics of the Velická Valley in the High Tatra Mountains, Slovakia. (45 hp)

587. Rettig, Lukas, 2020: Implications of a rapidly thinning ice-margin for annual moraine formation at Gornergletscher, Switzerland. (45 hp)
588. Bejarano Arias, Ingrid, 2020: Determination of depositional environment and luminescence dating of Pleistocene deposits in the Biely Váh valley, southern foothills of the Tatra Mountains, Slovakia. (45 hp)
589. Olla, Daniel, 2020: Petrografisk beskrivning av Prekambriska ortognejser i den undre delen av Särvskollan, mellersta delen av Skollenheten, Kaledonska orogenen. (15 hp)
590. Friberg, Nils, 2020: Är den sydatlantiska magnetiska anomalin ett återkommande fenomen? (15 hp)
591. Brakebusch, Linus, 2020: Klimat och väder i Nordatlanten-regionen under det senaste årtusendet. (15 hp)
592. Boestam, Max, 2020: Stränder med erosion och ackumulation längs kuststräckan Trelleborg - Abbekås under perioden 2007-2018. (15 hp)
593. Agudelo Motta, Laura Catalina, 2020: Methods for rockfall risk assessment and estimation of runout zones: A case study in Gothenburg, SW Sweden. (45 hp)
594. Johansson, Jonna, 2020: Potentiella nedslagskratrar i Sverige med fokus på Östersjön och östkusten. (15 hp)
595. Haag, Vendela, 2020: Studying magmatic systems through chemical analyses on clinopyroxene - a look into the history of the Teno ankaramites, Tenerife. (45 hp)
596. Kryffin, Isidora, 2020: Kan benceller bevaras över miljontals år? (15 hp)
597. Halvarsson, Ellinor, 2020: Sökande efter nedslagskratrar i Sverige, med fokus på avtryck i berggrunden. (15 hp)
598. Jirdén, Elin, 2020: Kustprocesser i Arktis – med en fallstudie på Prins Karls Forland, Svalbard. (15 hp)
599. Chonewicz, Julia, 2020: The Eemian Baltic Sea hydrography and paleoenvironment based on foraminiferal geochemistry. (45 hp)
600. Paradeisis-Stathis, Savvas, 2020: Holocene lake-level changes in the Siljan Lake District – Towards validation of von Post's drainage scenario. (45 hp)
601. Johansson, Adam, 2020: Groundwater flow modelling to address hydrogeological response of a contaminated site to remediation measures at Hjortsberga, southern Sweden. (15 hp)
602. Barrett, Aodhan, 2020: Major and trace element geochemical analysis of norites in the Hakefjorden Complex to constrain magma source and magma plumbing systems. (45 hp)
603. Lundqvist, Jennie, 2020: "Man fyller det med information helt enkelt": en fenomenografisk studie om studenters upplevelse av geologisk tid. (45 hp)
604. Zachén, Gabriel, 2020: Classification of four mesosiderites and implications for their formation. (45 hp)
605. Viðarsdóttir, Halla Margrét, 2020: Assessing the biodiversity crisis whitin the Triassic-Jurassic boundary interval using redox sensitive trace metals and stable carbon isotope geochemistry. (45 hp)
606. Tan, Brian, 2020: Nordvästra Skånes prekambriska geologiska utveckling. (15 hp)
607. Taxopoulou, Maria Eleni, 2020: Metamorphic micro-textures and mineral assemblages in orthogneisses in NW Skåne – how do they correlate with technical properties? (45 hp)
608. Damber, Maja, 2020: A palaeoecological study of the establishment of beech forest in Söderåsen National Park, southern Sweden. (45 hp)
609. Karastergios, Stylianos, 2020: Characterization of mineral parageneses and metamorphic textures in eclogite- to high-pressure granulite-facies marble at Allmenningen, Roan, western Norway. (45 hp)
610. Lindberg Skutsjö, Love, 2021: Geologiska och hydrogeologiska tolkningar av SkyTEM-data från Vombsänkan, Sjöbo kommun, Skåne. (15 hp)
611. Hertzman, Hanna, 2021: Odensjön - A new varved lake sediment record from southern Sweden. (45 hp)

LUNDS UNIVERSITET

Geologiska institutionen
Lunds universitet
Sölvegatan 12, 223 62 Lund